Ocean Sci. Discuss., https://doi.org/10.5194/os-2019-66-RC1,2019
© Author(s) 2019. This work is distributed under the Creative Commons Attribution 4.0License.

Ocean Science Discussions

Interactive comment on "Temporal evolution of Red Sea temperatures based on insitu observations (1958–2017)" *by* Miguel Agulles etal.

Anonymous Referee #1

Received and published: 27 August 2019

This work analyzes a large data set of temperature profiles obtained in the Red Sea from 1958 to 2017. The data sources are several data collections. The analyses are differentiated for three different areas: The northern and the southern Red Sea, and an outer area to the east of the Bad-el-Mandeb Strait. The analyses presented are quite exhaustive and include a description of the quality control process, the data interpolation method, and an inter-comparisons with model and SST satellite data. First the seasonal cycle of temperature for the different regions and depth ranges are analyzed and then the inter-annual and multidecadal variability is addressed.

In my opinion this work is very exhaustive and interesting. The main objectives of establishing the seasonal cycle of temperature as a function of the geographical location (Longitude/attitude) and depth, and studying the time variability at inter-annual

and multidecadal scales are achieved. The manuscript is well organized and, in general terms, well and clearly written. For all these reasons I believe it is suitable for publications with minor revisions.

We deeply thank the referee's comments and the effort he/she made in carefully reviewing our work. In the new version of the manuscript we have implemented all the points raised in the review. Thanks to those advices, the new version of the manuscript has been improved.

My main concern is the lack of an analysis of the salinity data. I assume that many of the available profiles analyzed come from CTD profiles or Argo profilers and therefore salinity data are also available. The analysis of temperature is very interesting by itself, but it would be much more complete if the companion salinity information was included. Note that the Red Sea is one the places of the world ocean with a highest evaporation and therefore the salinity variability and possible alterations could be of paramount importance. Furthermore, the dynamics of the circulation of the Red Sea would be driven by the density field (despite the wind-driven circulation). If the temperature changes are compensated by salinity changes then the density field is not altered. I think it would be important to know if this is happening or not. I am not an expert in the Red Sea circulation, but as long as I know, there is a thermohaline circulation and a water exchange with the Indian Ocean in order to compensate for the strong evaporation. Once again this depends on the density field and the joined action of temperature and salinity. Nevertheless, I understand that the role of the reviewer is to review the present work, not to suggest a different work. For this reason I consider this as a minor concern. The analysis of the temperature data merits publication by itself and I simply suggest that including a salinity analysis would improve very much the work.

Thanks for the comment. We also believe that salinity is important, but there have been several reasons for us to not include its analysis in this work. The number of salinity observations in the basin is significantly smaller than the temperature. At the same time, the correlation length scales for salinity are smaller than those of temperature (Llases et al, 2016), so more data would be required to obtain a reliable product. Additionally, including salinity would require specific tests to calibrate the algorithm, and to quantify the uncertainties, which would involve a huge extra effort. For all this, we have prefered to focus on temperature characterization,

specially considering that temperature has been recognized as the most influential factor for Red Sea ecosystems. We hope in the near future there will be enough salinity profiles thanks to the new observational systems that will allow us to produce an equivalent product for the salinity.

Other minor points. Introduction. Figure 1. For those people not familiarized with this region, a figure from a wider geographical area should be included in order to locate the Red Sea. Then, the present figure 1 could be a zoom from the larger area.

This figure has been modified in the paper.

At the beginning of the introduction (first paragraph), I miss a description of the Bad- al-Mandeb strait, mainly its maximum depth which I guess conditions the exchange between the Red Sea and the Indian Ocean. Otherwise, the introduction is clear and informative.

This information has been added in the first paragraph of the paper (L43).

Line 107: “the data has been quality controlled. . .”. It is true that the quality control is explained later in section 2.4, but the first time I read it I wondered how had been done the quality control?. Please, include a parenthesis (see section 2.4) for impatient readers likeme.

Thanks for the suggestion. The parenthesis has been included in the revised article.

Lines 116 and 117. This is the first time that OSTIA and ICOADS appear. Have this acronyms an explanation? Please, include it.

This has been updated in the revised article.

Line 120: “Both OSTIA products are merged after a cross validation is performed”. What kind of cross validation? How was it carried out? Please, explain it just a little.

That mergins is done by the OSTIA team. In particular, the cross validation of both OSTIA products is done estimating the bias in each product by calculating match-ups between each product and a reference data-set. The details of the procedure can be found in (Bell et al., 2000). This explanation has been added to the text (L121).

Line 143: “. . .to remove spikes, out layers and density inversions”. It is clear what a density inversion is, but the criteria to determine if a data point is an out layer is more subjective. Which criterion was been followed: two standard deviations from the mean value?, three?, those values beyond a certain percentile? Is the procedure the one explained in lines 150-155, or this is a different quality control? Why you use the 1% and 99% percentile criterion in some cases and the three standard deviations in other cases?

The paragraph that explain this part has been modified to better explain the quality control process. The quality control has been done in three steps:

Firstly, spikes and profiles with density inversions have been removed in all the area studied (Red Sea and outer region). Secondly, those profiles in the Red Sea showing temperatures colder than 20^{o}C below 500 m have been removed. This has been done because no temperature below 20ºC has been found in the reference KAUST dataset at any depth. Finally, as a third step, for the rest of the profiles (in the Red Sea and outer Region), those lying outside a range defined by three times the standard deviation are also rejected.

The 1% and 99% are used just for visualization of the range of values in the reference dataset, which have helped to identify the 20ºC threshold mentioned about. This has also been clarified in the text

Lines 185-190. I do not like very much these sentences. In Optimal Interpolation, the observations are considered as composed by a background field, a signal and an error, which is not necessarily a measurement error, but simply the part of the observation corresponding to a length scale on which we are not interested. The interpolated values are estimated using the statistics of the signal (variance and decaying scale) and the signal/error ratio. So I believe that “the weights are determined from the statistics of the observational errors” is not a good description.

In the original formulation of Optimal Interpolation (e.g. Gandin et al 1965) the weights of the background and the observations are defined in terms of the covariances of the background and observational errors. In the application of OI to atmosphere/ocean data those error covariances cannot be measured so they are defined using analytical formulations that involve a decay scale (e.g. Gaussian functions), and the error variance is substituted by the field variance. We agree that the original sentence in the manuscript was rather vague and we have corrected it. Now it reads:

“OI is an algorithm that estimates the optimal value of the field as a linear combination of available observations and a background (i.e. first guess) field, with weights determined from the covariances of observational and background errors”

Expression (1) could be improved. When writing in the left had side of the equation V(r) it seems to me that it is the value of variable V at the coordinate vector r (you say at a “given position r”). Then you say that BK is a M-vector. In that case V is also a vector, or r is a vector of positions.

The reviewer is right. In the left side of the equation 1 we have removed (r). The left side represents the analysed field which is a vector, not just a point in a given position.

In expression (5) Tij/T, I guess the exponent should be negative in the same way the exponent for the spatial correlation is negative. Otherwise the correlation increases with time,

The reviewer is right. We have corrected it. Thanks.

Figure 12. I would represent directly the values of the temperature for the climatology. In

that way you would know the temperature for each month of the year for the clima- tological cycle. In the present way, you have to look at the mean temperature and then add the anomaly. It is not very helpful. In line 345 and followings it is stated that the minimum anomaly for the seasonal cycle, and then the minimum temperatures along the year (it would be better to see temperatures directly) are found in August in the outer part. Taking into account that this area in to the north of 10°N, therefore in the northern hemisphere, it seems strange to the reader not familiarized with this region of the world that the minimum temperatures are reached in August, when one expect the maximum ones in the northern hemisphere. I think that this result needs some more explanations for the non-expert readers like me.

Before initial submission of the paper we had discussed a lot about how to present the seasonal variations. We had prepared both figures (for absolute values and for anomalies) and we had no clear preference as both options have pros and cons. Following the suggestion of the reviewer we have modified Figure 12, so it shows the absolute values.

Regarding the minimum values observed in the Gulf of Aden in summer, they are caused by the advection of cold waters from the Indian Ocean. The description of the detailed mechanism introducing that advection is out of the scope of the paper. Nevertheless we have introduce a sentence in the manuscript (L360) that reads:

"These results suggest that the relative minimum found in the Gulf of Aden during summer could be induced by the advection of cold waters from the Indian Ocean."

You compare sea temperature with air temperature at 1000 mbars, considered as the air in contact with the sea, and at 850 mbars. I think that using 850 mbar temperature makes no sense. The heat exchange between the sea and the atmosphere depends on the temperature of the air above it. If the air at 850mbar is very warm, but the air at the sea surface is cold, the cold air would enhance latent heat and sensible heat fluxes, no matter which is the temperature at 850 mbar. A different question is that 1000 and 850 mbar temperatures are very likely to be correlated, and therefore sea temperature and 850 mbar temperature are also correlated. My point is that we should not use time series to calculate correlations just because such time series are available. There must be some scientific reason. If you already have 1000 dbar temperature, please, do not use 850 dbar. It gives the false impression that there is some sort of phenomenon that can influence the sea temperature from the upper part of the atmosphere.

We appreciate your opinion, and we try to explain here our point. The 1000 mbar temperature is the one in contact with the sea, but it is well acknowledged that the sea temperatures also modify air temperatures at the air-sea interface. Therefore, correlations between SST and 1000 mbar temperatures could be due to oceanic effects on the atmosphere. That is the reason why we decided to use the 850 mbar temperatures, not because there were correlations. With that variable we intend to characterize the temperature of the air masses not affected by the air-sea interactions, as stated in the text (L508). By doing this, it is easier to interpret the correlations found: the changes in the temperature of the air (i.e. advection of air masses) is what drives the temperature in the Red Sea.

In line 373 you use the abbreviation std. I suppose it means standard deviation. Please, define it previously.

Done.

Some writing errors. Line 442: “the period cover by. . .” should be covered. Line 546. “the formal error from optimal interpolation have. . .” should be“has”.

This has been corrected

Interactive comment on Ocean Sci. Discuss., https://doi.org/10.5194/os-2019-66, 2019.

Ocean Sci. Discuss., https://doi.org/10.5194/os-2019-66-RC2,2019
© Author(s) 2019. This work is distributed under the Creative Commons Attribution 4.0License.

Ocean Science Discussions Open Access EGU

Interactive comment on “Temporal evolution of Red Sea temperatures based on insitu observations (1958–2017)” *by* Miguel Agulles etal.

Anonymous Referee #2

Received and published: 19 September 2019

This study investigates the temperature distribution in the Red Sea from observations collected from 1958 to 2017. The authors combine the data from multiple sources and apply a stringent quality control resulting in a high quality data set which is interpolated to produce a gridded climatology. This allows for an understanding of the Red Sea variability.

We are grateful to the referee for the constructive comments provided and the in depth reading of the present work. We have followed his/her suggestions, which we believe have helped to improve our manuscript.

As the observational data was collected from CTDs the article could have been greatly improved if the authors had included the analysis of salinity and done the calculations along density isopycnals rather than on depth surfaces.

Thanks for the comment. We also believe that salinity is important, but there have been several reasons for us to not include its analysis in this work. The number of salinity observations in the basin is significantly smaller than the temperature ones. At the same time, the correlation length scales for salinity are smaller than those of temperature (Llases et al, 2016), so more data would be required to obtain a reliable product. Additionally, including salinity would require specific tests to calibrate the algorithm, and to quantify the uncertainties, which would involve a huge extra effort For all this, we have prefered to focus on temperature characterization, specially considering that temperature has been recognized as the most influential factor for Red Sea ecosystems. We hope in the near future there will be enough salinity profiles thanks to the new observational systems that will allow us to produce an equivalent product for the salinity.

Furthermore the temperature used needs to be either Conservative Temperature or potential temperature not in situ temperature.

The reviewer is right and in fact potential temperature has been used. By in-situ we aimed at differentiating the in-situ observations from the satellite observations used afterwards. We have included the term “potential temperature” in the first paragraph of section 2.1.

I was surprised by the high percentage of the observations data was located incorrectly,

are the authors sure there is not a salinity compensation to this low temperature water that produces an appropriate density for this region.

Thanks for your appreciation. We had carefully checked that extent prior to discarding those profiles, but we are sure that there is no salinity compensation.

Overall I found the paper to be well written and is interesting and I believe it should be published. It is great that the authors made TEMPERSEA freely available.

Thank you very much. The product will be made freely available at PANGEA repository once the paper is accepted by the journal.

Interactive comment on Ocean Sci. Discuss., https://doi.org/10.5194/os-2019-66, 2019.

()Ocean Sci. Discuss.,
https://doi.org/10.5194/os-2019-66-RC3, 2019
© Author(s) 2019. This work is distributed under
the Creative Commons Attribution 4.0 License.

Ocean Science Discussions

Interactive comment on "Temporal evolution of Red Sea temperatures based on insitu observations (1958–2017)" *by* Miguel Agulles et al.

Anonymous Referee #3

Received and published: 9 October 2019

This paper takes generally available in situ temperature profile data for the Red Sea and Gulf of Aden, combines it with newly available data to create long-term climatological mean fields of surface and subsurface temperature as a baseline for time series of month/year temperature fields (surface and subsurface) for all months for years 1958-2017. Error estimates are calculated from subsampled GLORYS reanalysis data. Some discussion of season, interannual, and decadal variability is included, with decadal trends of opposite sign at the surface and at 125 m depth.

This work is definitely of interest, both for the climatological mean fields of temperature in the Red Sea and Gulf of Aden, and for the analysis of seasonal to decadal changes in the temperature field, with their influence on the climate and biota of the region. The authors write very clearly regarding the method used, with a particularly

nice explanation of optimal interpolation and of the calculation of error statistics. A more thorough examination of the data would improve the paper, as would validation of the subsurface long-term mean fields against existing products, and more discussion of results, particularly trends of opposite sign at different levels in the water column. Details below.

We thank the reviewer for his/her overall positive evaluation. In the following we try to address all the his/her comments.

First, the addition of the KAUST data set is a welcome augmentation of existing data for the Red Sea, especially with the possibility of continued monitoring by this source. I do not know the data policy for this journal, but the data used within the paper should be publicly available for reproducibility. The authors should note in the paper where the data can be obtained.

The final product will be made freely available in the Pangea repository once the

paper is accepted. This sentence is added at the end of the paper, in the acknowledgments section.

Figure 2 shows a rather startling distribution of temperature values in the Red Sea, especially with what appears to be a very large number of profiles with temperatures well outside the range of Red Sea temperatures at deeper depths. It would be a great service if the authors could detail the data a little more especially those which they state must have erroneous positions. This would help users (and maintainers) of CORA and similar data sets to examine and either flag or correct the erroneous data. Did the authors use CORA quality flags? Did these erroneous data have CORA quality flags?

Yes, we used the CORA quality flags to discard suspicious profiles. Specifically, we downloaded quality flags related to temperature and depth and only kept those profiles flagged with a value of 1 (Good data). It must be said that as a previous control we also tried to keep observations with flags equal to 2 (Probably good data), with the intention of applying a postprocessing, but this approximation does not increased the number of good profiles. Therefore, we decided to use the more restrictive selection keeping only profiles flagged as "Good Data".

Regarding the control of erroneous positions, CORA quality control process considers "bad location" those profiles on land positions (positions more than 5km distant from nearest coastline with elevation above 50m). As you can see in the next figure (Figure 1-RC3) for the Red Sea, no observations are located on land, so CORA flags were not available to identify the mislocation of the profiles we have discarded.

The full description of CORA database flags are obtained from (http://resources.marine.copernicus.eu/documents/QUID/CMEMS-INS-QUID-013-001b.pdf).

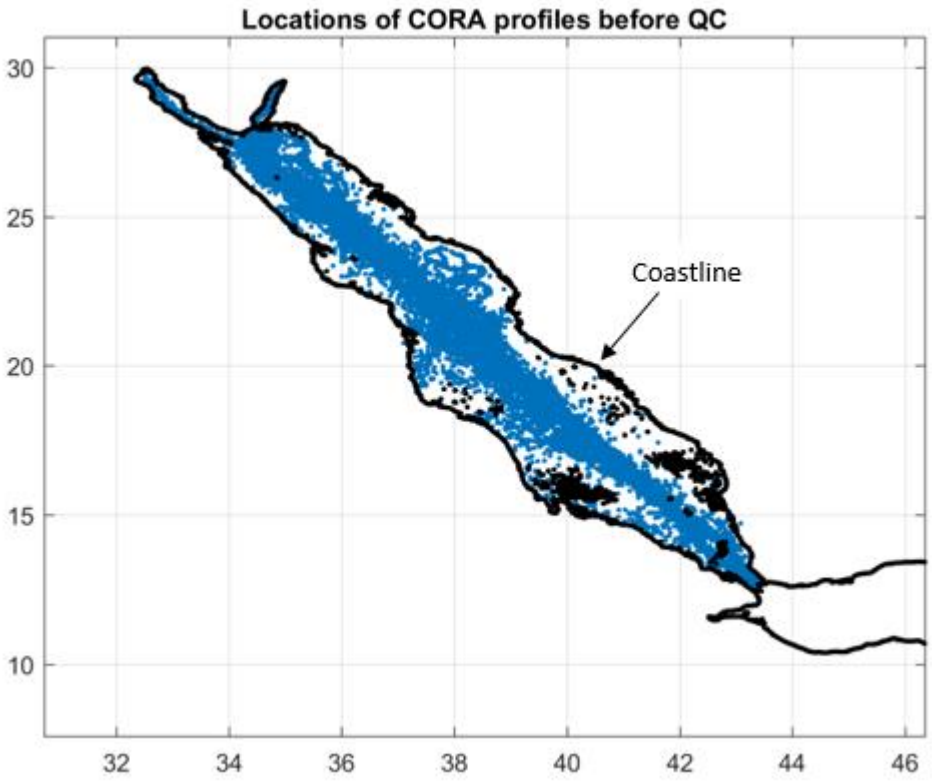

Figure 1-RC3

Figure 7shows a patter of RMSE Glorys vs. climatology (and optimal algorithm) that appears suspicious - with what looks like the exact same pattern in the 1960s, 1980s, and 2000s centered at 1000 m with the intermittent decades showing near zero error. Can the authors explain this?Is it some kind of decadal cycle embedded in Glorys, rendering it maybe less than useful for error analysis?

The reviewer is right noticing this periodicity in the diagnostic. The reason is that, in order to obtain RMSE Glorys Vs Optimal Algorithm (Figure 7b in the paper) we needed to extract the observation locations of observations for the whole period of CORA (60 years, 1958-2017), but Glorys record is only 23 years long (1993-2015). Therefore, we concatenate the 23 years of Glorys till

cover the time of observations, so we can extract the CORA locations for the whole period. It must be noted that we do not really care about the actual values of Glorys. We only use it as a synthetic reality so we can test the impact of the mapping procedure.

It also might be nice to enlarge the upper few hundred meters where the largest errors are found, but hard to see in the full vertical graphic.

We thank the reviewer for the suggestion. We have modified the vertical axis of Figure 7 to increase the zoom in the upper layer.

The long-term climatological mean field is discussed at length, but only validated with a comparison with AVHRR at the surface. It should be compared at subsurface depths to the World Ocean Atlas 2018 (WOA18) field, which are on the same grid size (0.25 x

0.25) and over nearly the same time period (1955-2017) - or another widely used long- term global climatological mean field. This comparison could yield some interesting results as to the efficacy of concentrating on a specific region, instead of using a region of a global climatology, with attendant extra attention, quality control, and in this case new data sources.

Thank you for this suggestion, the comparison with another widely used product is really worth to be done. We have checked the availability of WOA18 database but just climatology fields are available at the repository. Therefore we have compared our TEMPERSEA product with another well-known hydrographic gridded product used in the IPCC reports (Ishii et al., 2003) In spite of having coarser spatial resolution (1º), it provides monthly field temperatures from 1955 to 2012, thus allowing a more in –depth comparison for the common period.

Several diagnostics have been computed. First, we compare the annual mean temperature at three different depths (at surface, at 125m and 325 m of depth), both for the Red Sea and the Gulf of Aden (Figure 2-RC3 and Figure 3-RC3). It can be seen that both products are highly correlated in the upper layer, while they differ much more in the subsurface layers. This is also confirmed by the second diagnostic, the spatially averaged RMS difference computed each month for the whole domain (Figure 4-RC3). There is a clear maximum in the RMSD at 125m. Unfortunately, there is not independent data that could be used to decide which product is more accurate. Therefore, we have decided to not include this comparison in the paper as we are not able to show the added value of the product.

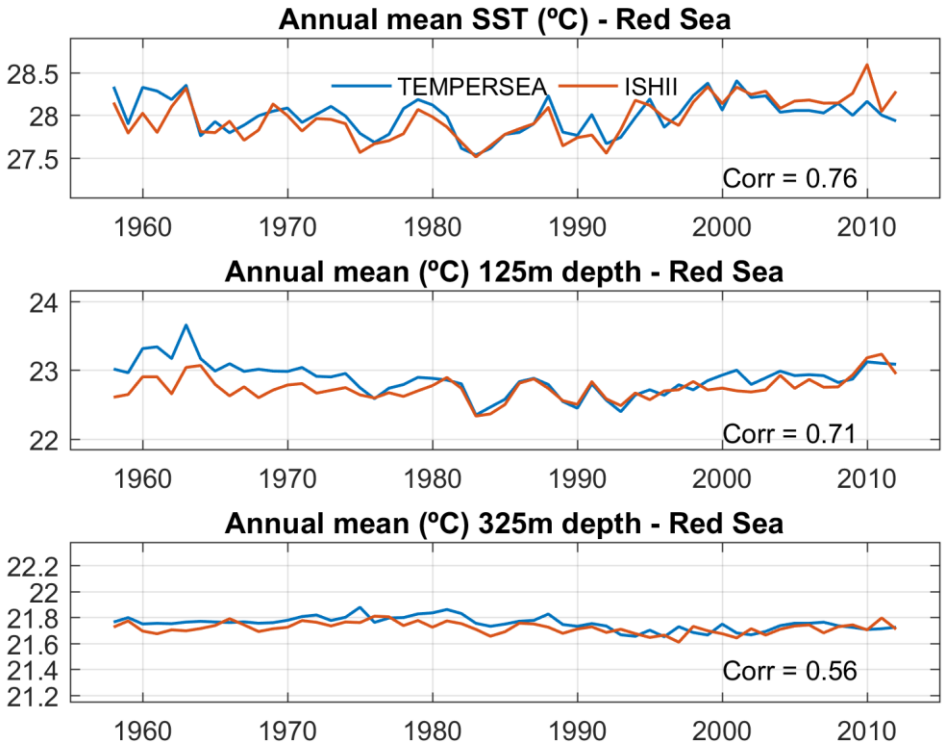

Figure 2-RC3

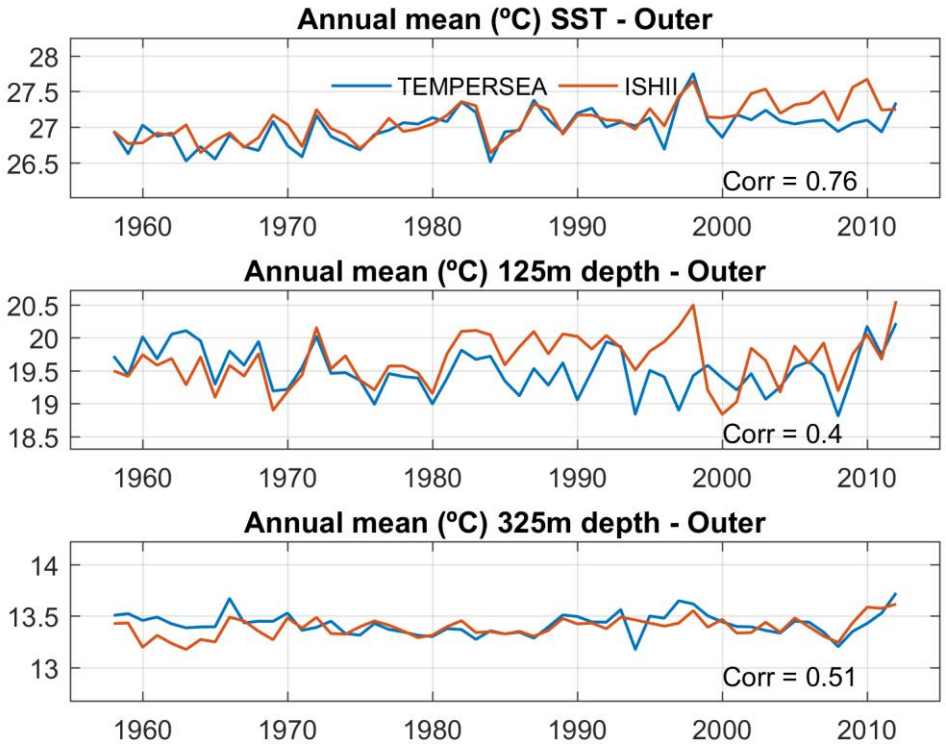

Figure 3-RC3

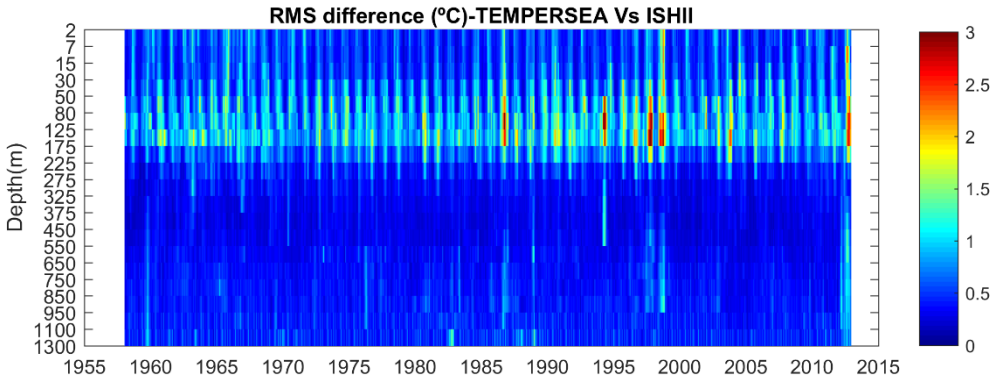

Figure 4-RC3

Grid size - sampling strategy: is a 0.25 x 0.25 degree grid really necessary to capture temperature change in the Red Sea? According to the authors discussion, less than 10 temperature profiles per month are necessary to adequately quantify temperature change in the Red Sea. If that is truly the case, would not a 1.0 x 1.0 grid along the axis of the Red Sea be sufficient to capture temperature change?

To better define the changes of the temperature along the abrupt coast of the Red Sea and his characteristic strait in the South, it is necessary to work with a relatively fine grid. Even if the final structures have large characterisic length scales, we prefer to provide the data in a way that properly capture the coastlines. Moreover, there is another mathematical reason. If the characteristic length scales are about 100-150km (as computed from the Glorys data), we need at least 4 grid points to properly capture those structures, so 0.25º is the minimum resolution to be in the safe side.

In figure 4, it is very hard to see the grid structure used - is there another way to represent it? Maybe just in black and white rather than color?

Thanks for the suggestion, we have modified the figure in the paper.

But assuming there are multiple grids laterally across the Red Sea at each latitude, it appears that the K-mean algorithm aggregates data into one or sometimes two grid areas across the Sea longitudinally (Figure 5). These appears to lose any advantage of a 0.25 x 0.25 grid resolution. It may be due to the graphic, but the authors should spend some more time discussing the importance of the 0.25 x 0.25 grid resolution to this work.

We think the reviewer has misinterpreted the figure. The goal of the K-means is to reduce the number of observations at the time of computing the background field. We do that clustering them, so we can remove points that would provide redundant information for the computation of the climatology. Then, the spatial analysis for the background field is performed on the standard 0.25º grid. For the monthly analysis the number of observations is much reduced so we can use all of them in the mapping procedure and take advantage of the periods/locations when/where there are many observations.

Time frequency: similarly, what is the advantage of the month/year time frequency (12 monthly temperature fields in the Red Sea per year 1958-2017)? As the authors note (with the term "surprisingly" though I dont think it should be surprising to the authors who are familiar with historic measurement strategies in the Red Sea) there are many months without any data at all in the Red Sea, and other months with very few measurements. Seasonal temperature cycle in the Red Sea is examined from a climatological (long-term) perspective. I dont see any particular explanatoin of the advantage to month/year fields over simple yearly fields in quantifying and discussing interannual and decadal variability, especially for data sparse years. The authors should do a little more explanation of why monthly fields are produced. At the least a matrix of coverage (or lack thereof) for each month/year should be presented graphically. This would give

a better understanding of data sparsity influence on error, as a companion to figure 21.

Even if in our analysis we only make advantage of the monthly fields when computing monthly std variability, we strongly believe that it is better to provide the product at the highest time resolution. Then, the users could decide at which level would they like to aggregate the data. It has to be kept in mind that during some periods there were enough profiles to accurately characterize monthly variations as can be seen in the following figure (Figure 5-RC3). In the product the periods of better quality are reflected in the error maps and error time series as discussed in the text.

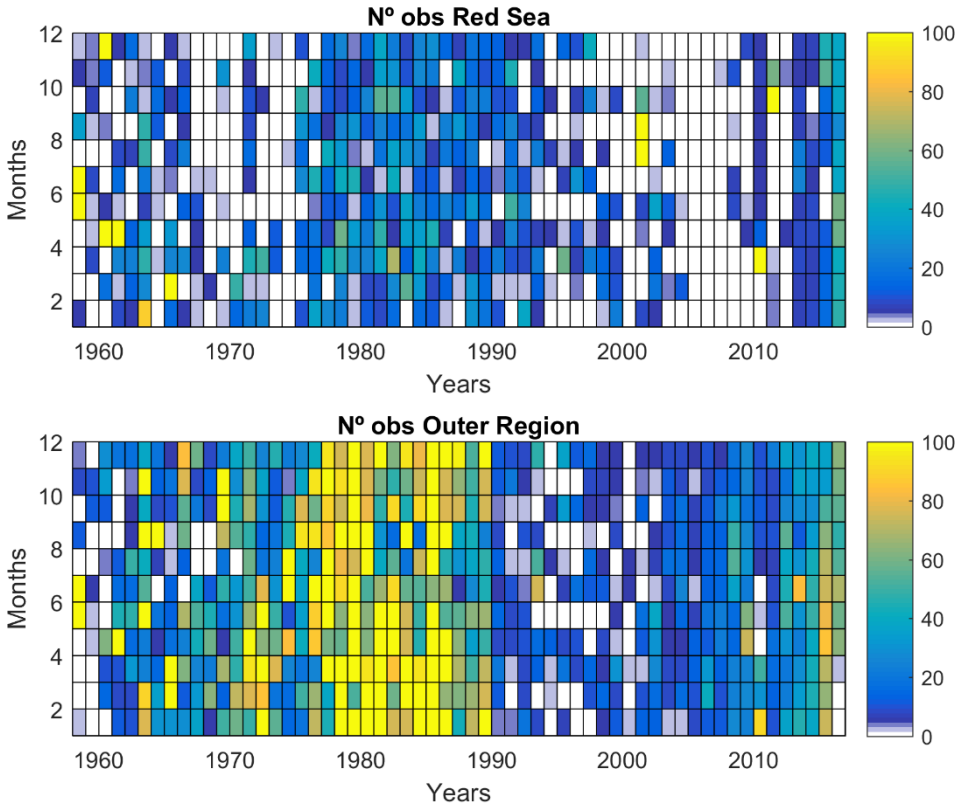

Figure 5-RC3

In discussing results, the authors note that most interannual variations in the upper layer of the Red Sea can be explained by large scale changes in the air temperature. This is not completely convincing. There is a good correlation, but isnt it equally as likely that it is the air temperatures influenced by the upper ocean temperature rather than the other way round?

Short wave radiation as well as trapped long wave radiation is absorbed by the ocean surface and radiated back at a slower rate to the lower atmo- sphere. A little more discussion would be needed to convince that it is large scale air temperature which is the major factor in the upper ocean.

When preparing the first version of the manuscript we had a thorough discussion with atmosphere scientists about this issue. They suggested to use air temperature at 850mbars (roughly 1500 m height) to ensure that the ocean feedbacks are minimized. We agree that the sea has an effect on the air temperature, but this is restricted to the lower layers. Air temperature at 850 mbars (1500 m height) is too far from being significantly affected by the sea temperature of a small region like the Red Sea. In the manuscript we have added a sentence clarifying that 850mbars correspond to 1500m height. Also we discuss the correlation with air temperature at two heights, close to the sea surface (1000 mbars) and at 850 mbars, showing that correlations are higher close to the sea surface due to the air-sea feedbacks, but that correlations with temperature at 850 mbars is still very high.

One of the remarkable features the authors find is that upper ocean temperatures are increasing (decadally) but lower depths are decreasing. How can this be if the main factor in the temperature change is air temperature, and there is little exchange with any water source outside the Red Sea? It may be that the answer has to do with the interannual change in the depth of the thermocline.

Figure 14 shows thermocline depth seasonal change. Thermocline depth in the south is fairly constant over the year, but changes in the north. If the thermocline were to shallow in February say, cooler water would be higher in the water column and heating would be concentrated closer to the surface, creating the opposite sign trend pattern with depth shown by the authors. This is speculation, but it would be worth a bit more investigation by the authors to validate and maybe explain the change in sign for decadal trend.

We don't really have an explanation for this discrepancy between the long term evolution of both layers, and it is out of the scope of the paper to run a full analysis on

this interesting issue. Regarding the interannual change in the depth of the thermocline we do not understand why that would explain the long term discrepancies between layers, as the thermocline depth is a diagnostic, not a mechanism.

Small things

- line 98: what does "delayed mode" mean here? - lines 116, 117, if OSTIA and ICOADS are acronyms, they should be defined. - line 132, "sea-ice concentration" maybe could be removed. GLORYS may assimilate but it is irrelevant in the Red Sea. Thanks for the comments. We have updated the paper with those corrections.

it would be nice, in figure 3 to give some indication of the data which came from KAUST as opposed to CORA.

We have included a dashed line in Figure 3 to indicate the observations coming from KAUST.

- line 204, add space between "as" and gamma. - line 206, "pof" should be "of"

Thanks for identifying the typos, they have been corrected (L213 and L215).

- lines 315-317, why would satellite data from the top mm of the water

column have a larger variability than in situ data from 2-4 m?

It is stated in the manuscript that the product is representative of the first 4 m of the water column. Therefore, one can expect that that fraction of the water column is less responsive to changes in the forcing that the first mm of the water column (as it involves more mass). Consequently the variability is somehow damped.

- line 412, "imposed to" should be "imposed on" - lines 493-494, lateral advection seems to play an important role..." replace "seems to play" with "plays" if there is actual evidence for this. - line 561, "specially" should be "especially"

Thanks, these have been corrected.

- lines 565-566, "Our results show that multidecadal variations have been important in the past and can bias high the trends from 30-40 years of data." How can multidecadal trends, presumably a cycle, bias high trends? Are the authors referring to multidecadal trends which are not fully represented in 30- 40 years?

Yes, this is exactly what we mean. Multidecadal variations (not trends) not fully represented by the 30-40 years of data can enhance/reduce the underlying long term trends.

It appears from figure 19 that this could be so in this specific case, but as a generality a partial cycle could bias trends either high or low. Authors should either remove "high" or refer specifically to the Red Sea trend.

We agree, we have removed the adjective “high”

Interactive comment on Ocean Sci. Discuss., https://doi.org/10.5194/os-2019-66, 2019.

Ocean Sci. Discuss., https://doi.org/10.5194/os-2019-66-SC1,2019
© Author(s) 2019. This work is distributed under the Creative Commons Attribution 4.0License.

Ocean Science Discussions Open Access EGU

Interactive comment on “Temporal evolution of Red Sea temperatures based on insitu observations (1958–2017)” *by* Miguel Agulles etal.

Cheriyeri Poyil Abdulla

abducps@gmail.com

Received and published: 5 September 2019

Interactive comment on the work entitled “Temporal evolution of Red Sea temperatures based on in situ observations (1958–2017)” is listed below and attached as a file along with this. (by C P Abdulla).

Appreciating the authors for the work entitled “Temporal evolution of Red Sea tempera- tures based on in situ observations (1958–2017)” by Miguel Agulles et al., 2019 which has analyzed the in situ profiles in the region and developed a gridded product based optimal interpolation technique. The article further discussed the seasonal, interannual and decadal signal in the temperature of the Red Sea and outer region (mainly Gulf of Aden).

We deeply thank the referee’s comments and the effort hemade in reviewing carefully our work. In the new version of the manuscript we have implemented all the points raised in the review.

My major concern is on the analysis and some of them are listed below.

Comment 1: Please add in the text about the criteria used for removing the spikes, out layer and density inversion.

The paragraph that explain this part has been modified to better explain the quality control process. As a brief explanation, the quality control has been done in three steps:

Firstly, spikes and profiles with density inversions have been removed in all the area studied (Red Sea and outer region). Secondly, those profiles in the Red Sea showing temperatures colder than 20^{o}C below 500 m have been removed. This has been done because no temperature below 20ºC has been found in the reference KAUST dataset at any depth. Finally, as a third step, for the rest of the profiles (in the Red Sea and outer Region), those lying outside a range defined by three times the standard deviation are also rejected.

Comment 2: In Figure 2, why is the left panel the out data are plotted, it would be better to keep only the Red Sea data to cope with the caption of the Figure

Thank you for your comment. We have discussed about this but we think useful for the reader to see the large amount of misplaced profiles existing in the CORA dataset to better understand the quality control applied.

Comment 3: Figure 5 shows the distribution of all the available observations for January in the region and the profiles distribution after applying the K-means algorithm.

That is correct.

Are these profiles shown in (Figure 5b) the only profiles used in Optimal Interpolation?

Yes, they are. Prior to run the algorithm to obtain the background fields, we have carried out some tests to know the minimum number of observations required to get the analysis field. As you point out, in Figure 5b there are 135 profiles to obtain the background of January. If we had used more profiles, the computational cost (the inversion of the covariance matrix between observations) would have been higher to obtain basically the same result.

Comment 4: When I check the data availability in the Red Sea region from World Ocean Database, the data points are mostly aligned along the center with significantly lower number profiles towards both eastern and western coast. To what extent the second source of data cover this in space and time?

Thank you for your appreciation. In fact, we spent some time comparing WOD data and CORA data while preparing the manuscript. In order to clarify this aspect, we attached two figures below (Figure 6-SC1 and Figure 7-SC1). The first one compares the number of observations between both datasets for three different years. The second figure shows the number of observations per year in both datasets. It can be seen that CORA includes more profiles and a better coverage than WOD.

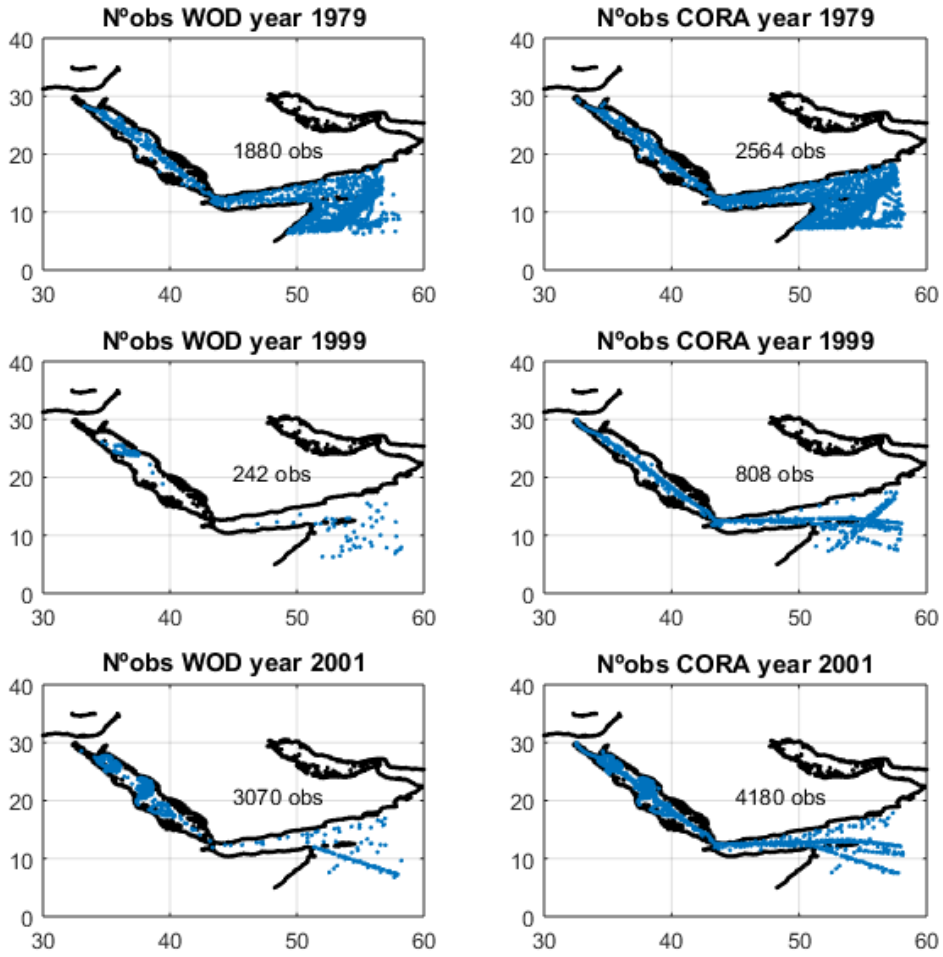

Figure 6-SC1

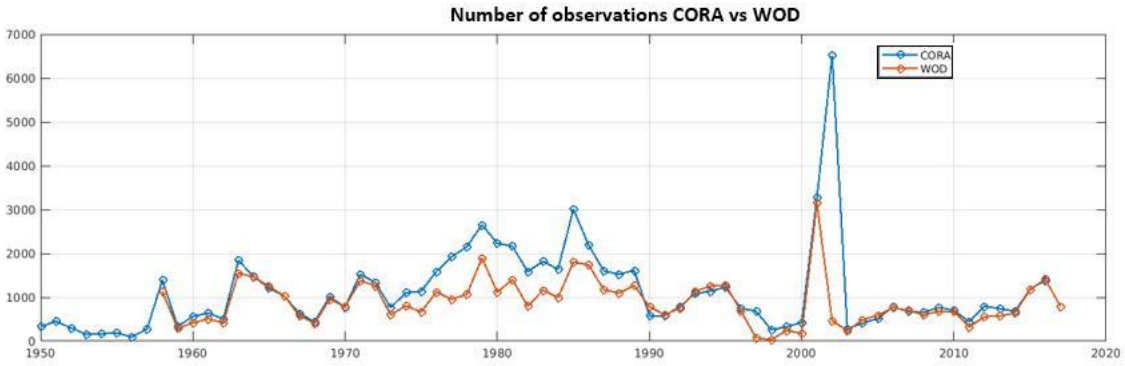

Figure 7-SC1

Comment5: The 3D gridded temperature product spanning for the period 1958-2017 is will be very helpful in understanding the Red Sea. From my understanding of the manuscript, I found that the amount of profiles in the Red Sea used for the analysis is very low, except for 2 or 3 years (1959, 2000 and 2016). If this is true, is the derived product will be reliable to discuss interannual and decadal signal?

We believe the product is reliable to assess the interannual and decadal signal. First, we have to say that the number of observations is not the only thing that matters, as the spatial distribution of those observations is also very important (i.e. with less than 10 profiles one can obtain a good representation of the large scale patterns if they are well placed). Second, the Optimal Interpolation algorithm also produced an estimate of the error associated to each analysis field depending on the number of observations and their spatial distribution (.ie. the formal error). We deliver that formal error along with the TEMPERSEA product. This

can help to identify the periods when the product is less reliable and to quantify those errors.

In the discussion section we show that 10 observations per month in the Red Sea would be enough to do a reliable mapping (see Fig 21). Moreover, to reinforce the confidence in the product we compare the results with two source of satellite data and the results are within the error bar (see Fig 10)

Comment 6: A table explaining the number of profiles used in the OI per each decade separately in the Red Sea will be helpful to show the data distribution in the Red Sea (which is the prime focus of the study) used in the analysis in addition to a map showing the data spread can be added as supplementary file.

We think that separating the number of observations per decade would not provide any new information as in Figure 7-SC1 we represent the number of observations per year. In order to clarify your question, see below the Figure 8-SC1 and Table 1-SC1 which show the number of observations per decade in the Red Sea and the outer region separately. Nevertheless, we emphasize that what it is important to evaluate the reliability of the product are the number and distribution of the observations per month. So, using the number of profiles per decade would not produce a reliable estimate of the product accuracy. Instead, the most accurate approach to assess the reliability of the product is to use the formal error. It is also included in TEMPERSEA product and will be made freely available at PANGEA repository once the paper for publication.

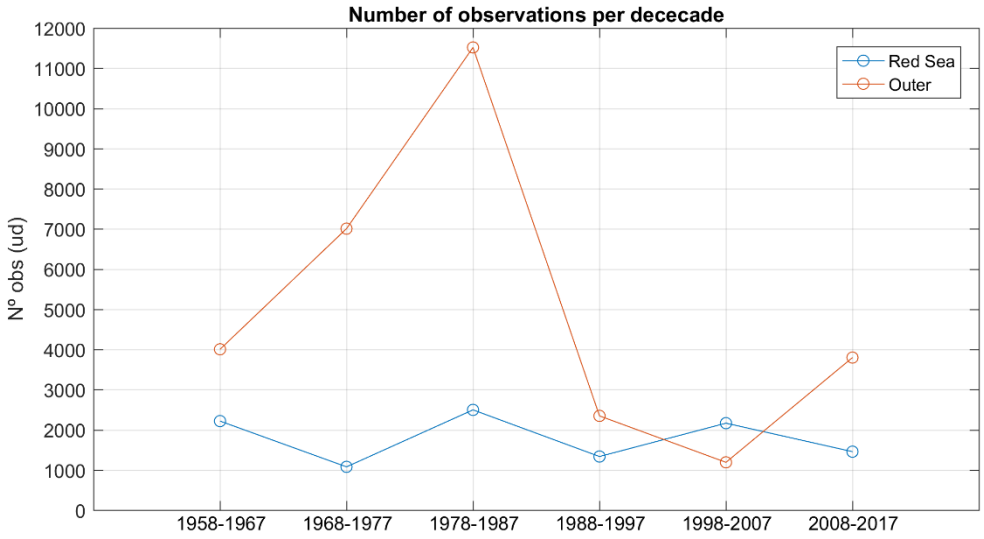

Figure 8-SC1

Nº obs/10years	Red Sea	Outer
1958-1967	2218	4017
1968-1977	1079	7018
1978-1987	2497	11531
1988-1997	1336	2349
1998-2007	2166	1191
2008-2017	1457	3800
Total Nº obs	10753	29906

Table 1-SC1

Comment 7: Most of the data represent the outer region and few only represent the Red Sea, so the title of the manuscript and the name of the product should consider that.

.

We thank the reviewer for the comment. Our main interest is the Red Sea and we use the outer data to put Red Sea variability in context. Nevertheless, we accept the reviewer's suggestion and have modified the title of the paper which now reads:

"Temporal evolution of temperatures in the Red Sea and the Gulf of Aden based on in-situ observations (1958-2017)"

Please also note the supplement to this comment:
https://www.ocean-sci-discuss.net/os-2019-66/os-2019-66-SC1-supplement.pdf

Interactive comment on Ocean Sci. Discuss., https://doi.org/10.5194/os-2019-66,2019.

Temporal evolution of ~~Red Sea~~ temperatures in the Red Sea and the Gulf of Aden based on in-situ observations (1958-2017)

Miguel Agulles[1], Gabriel Jordà[1,2], Burt Jones[3], Susana Agustí[3], Carlos M. Duarte[3,4]

[1]Instituto Mediterráneo de Estudios Avanzados (UIB-CSIC), Esporles, Spain
[2]Centre Oceanogràfic de Balears. Instituto Español de Oceanografía. Palma, Spain
[3]Red Sea Research Centre (RSRC), King Abdullah University of Science and Technology, Thuwal 23955, Saudi Arabia
[4]Computational Bioscience Research Center (CBRC), King Abdullah University of Science and Technology, Thuwal 23955, Saudi Arabia

Abstract. The Red Sea holds one of the most diverse marine ecosystems in the world, although fragile and vulnerable to ocean warming. Several studies have analysed the spatiotemporal evolution of the temperature in the Red Sea using satellite data, thus focusing only on the surface layer and covering the last ~30 years. To better understand the long-term variability and trends of the temperature in the whole water column, we produce a 3D gridded temperature product (TEMPERSEA) for the period 1958-2017, based on a large number of in situ observations, covering the Red Sea and the Gulf of Aden. After a specific quality control, a mapping algorithm based on optimal interpolation has been applied to homogenize the data. Also, an estimate of the uncertainties of the product has been generated. The calibration of the algorithm and the uncertainty computation has been done through sensitivity experiments based on synthetic data from a realistic numerical simulation.

TEMPERSEA has been compared to satellite observations of sea surface temperature for the period 1981-2017, showing good agreement specially in those periods with a reasonable number of observations were available. Also, very good agreement has been found between air temperatures and reconstructed sea temperatures in the upper 100 m for the whole period 1958-2017 enhancing the confidence on the quality of the product.

The product has been used to characterize the spatio-temporal variability of the temperature field in the Red Sea and the Gulf of Aden at different time scales (seasonal, interannual and multidecadal). Clear differences have been found between the two regions suggesting that the Red Sea variability is mainly driven by air-sea interactions, while in the Gulf of Aden, the lateral advection of water also plays a relevant role. Regarding long term evolution, our results show only positive trends above 40 m depth, with maximum trends of 0.045 + 0.016 ºC decade-1 at 15 m, and the largest negative trends at 125 m (-0.072 + 0.011 ºC decade-1). Multidecadal variations have a strong impact on the trend computation, and restricting them to the last 30-40 years of data can bias high the trend estimates.

1 Introduction

The Red Sea is a narrow basin, meridionally elongated (2250 Km), lying between the African and the Asian continental shelves, and extending from 12.5 °N to 30 °N with an average width of 220 Km (Figure 1~~Figure 1~~). It is a semi-enclosed basin connected to the Indian Ocean through the Bab-al-Mandeb Strait, with a still depth of 137m (Werner and Lange., 1975), at the south and to the Mediterranean Sea through the Suez Canal at the north. The bathymetry is highly irregular along the basin, with a relatively shallow mean depth (524 m; (Patzert, 1974), but with maximum recorded depths of almost 3.000 m. At its northern end, it bifurcates into two gulfs, the Gulf of Suez on the West with an average depth of 40 m and the Gulf of Aqaba on the East with depths exceeding 1.800 m (Neumann and McGill, 1961).

The transport through the Suez Canal, which connects the Mediterranean Sea with the Gulf of Suez and the Red Sea, is relatively small, and therefore, the only significant connection between the Red Sea and the global ocean is the Strait of Bab-al-Mandeb (Sofianos et al., 2015). There, a two layer system is established in which relatively fresh and cold waters flow from the Indian Ocean into the Red Sea in the upper layer while saltier and warmer waters flow outside in the lower layer . Due to its arid setting, the Red Sea experiences one of the largest evaporation rates in the world, which in combination with its semi-enclosed nature leads to high salinities across the whole basin (Sofianos et al., 2015). The hydrodynamic characteristics are strongly influenced by the wind forcing with different seasonality. The seasonal winds blow south-eastwards in the northern part of the basin through the whole year, but in the southern region, the winds reverse form north-westerly in summer to south-easterly in winter under the influence of the two distinct phases of the Arabian monsoon, (Patzert, 1974; Sofianos, 2015).

The Red Sea holds one of the most diverse marine ecosystems in the world, although fragile and vulnerable to ocean warming (Thorne et al., 2010). Water temperature plays a key role in ecosystems evolution, which are usually adapted to the environmental thermal range. Marine species respond to ocean warming by shifting their distribution poleward and advancing their phenology (Poloczanska et al., 2016). While parts of the ocean may be warming gradually, others may experience rapid fluctuations, inducing more significant impacts on biodiversity. Impacts of warming are likely to be greatest in semi-enclosed seas, which tend to support warming rates higher than the global ones (Lima and Wethey, 2012), as documented for the Red Sea (Chaidez et al., 2017).

Several recent studies have analysed the spatiotemporal evolution of the temperature in the Red Sea using satellite data from AVHRR (Advanced Very High-Resolution Radiometer), thus focusing only on the surface layer and covering from early 1980's onwards. Those studies have identified a warming trend with values ranging from 0.17 ºC decade-1 to 0.45 ºC decade-1 across the basin for the period 1982-2015 (Chaidez et al., 2017). Also, sea surface temperature exhibits a strong interannual variability (Eladawy et al., 2017) which is mainly driven by the air temperature (Raitsos et al., 2011). However, these studies are

limited to ~30 years due to the observational period of remote data. Also, although the evolution of surface conditions is very relevant, the temperature variability in the whole water column has effects on marine biota (Bongaerts et al., 2010), so products based on depth-resolving in situ observations better reflect the thermal regime across the ecosystem than sea surface trends alone.

Global hydrographic products like EN4 (Good et al., 2013) or ISHII (Ishii and Kimoto, 2009) that interpolate in-situ observations to create a monthly 3D product for the last decades are available. However, those products have low spatial resolution (~1º) and the quality controls applied are not region specific, which cast doubts on their accuracy in the narrow Red Sea. In order to overcome the limitations satellite products and global hydrographic products have, and to be able to characterize the spatiotemporal variability of the 3D temperature field to inform research on the thermal ecology and variability of Red Sea ecosystems, a dedicated regional observational product is required.

Here we produce a gridded temperature product for the period 1958-2017 at monthly resolution as a resource to describe the evolution of the Red Sea temperature during the last six decades and underpin research on the impacts of ocean warming across the Red Sea. The product covers the Red Sea and the Gulf of Aden with a spatial resolution of 0.25°x 0.25°. This product is based on the assimilation and reanalysis of a large number of in situ observations collected in the region. After a specific quality control, a mapping algorithm has been applied to homogenize the data. Also, an estimate of the accuracy of the product has been generated to accurately define the uncertainties of the product. We then use the product to characterize the seasonal, interannual and multidecadal variability of the 3D temperature field in the Red Sea and the Gulf of Aden.

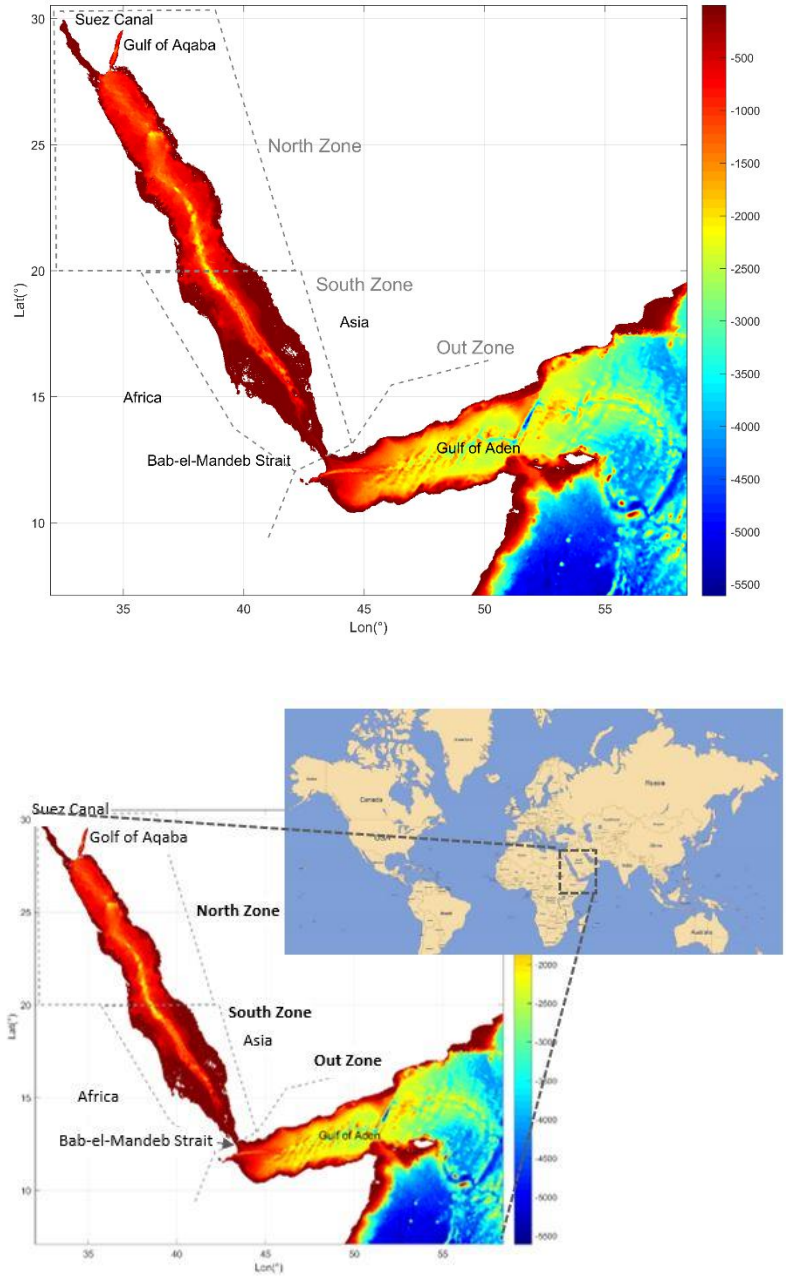

Figure 1: Domain and bathymetry of the region included in the TEMPERSEA product. The three zones used in the presentation of results (North, South and Outer) are identified by grey lines. (data source: https://www.gebco.net/data_and_products/gridded_bathymetry_data).

2 Data and Methods

2.1 In situ data

In situ potential temperature observations were obtained from two databases. The first one is CORA (Cabanes et al., 2013), a delayed mode product (the April release corresponds to profiles dated up to June

of the n-1 year) designed to feed global reanalyses. CORA covers the global ocean from 1950 to 2016 and integrates quality controlled historical profiles from several data collections (Argo, GOSUD, OceanSITES and World Ocean Database). The details of this database can be found in http://www.coriolis.eu.org/Science2/Global-Ocean/CORA and it is freely delivered by the Copernicus Marine Service (http://marine.copernicus.eu/services-portfolio/access-to-products/?option=com_csw&view=details&product_id=INSITU_GLO_TS_REP_OBSERVATIONS_013_001_b).

The second source of data is the database collected by King Abdullah University of Science and Technology (KAUST), from 2010 to 2018. It includes all the data collected by KAUST in the Red Sea through different platforms (floats, ships, gliders, Argo). The data has been quality controlled (see section 2.4) with specific criteria for the Red Sea and will be used here as the reference dataset, (Karnauskas and Jones, 2018).

2.2 Satellite data

Two sources of remote sensed sea surface temperature (SST) data are used. The first dataset is obtained from the National Ocean and Atmosphere Agency (NOAA) and is based on AVHRR (Advanced Very High-Resolution Radiometer) over the period 1981 -2017. These data have a spatial resolution of 0.25°x0.25°, and can be obtained at monthly temporal resolution from the National Center for Environmental Information (NCDC-NOAA, ftp://ftp.ncdc.noaa.gov/pub/data/).

The second source of data is OSTIA(Operational SST and Sea Ice Analysis), a global product generated by UK Met Office (Roberts-Jones et al., 2012). OSTIA merges in situ data from the ICOADS dataset (International Comprehensive Ocean-Atmosphere Data Set, more information https://icoads.noaa.gov/) with satellite data from infra-red radiometers over the period of 1985 to 2007. The dataset has a spatial resolution of 0.25°x0.25° and monthly temporal resolution, (http://marine.copernicus.eu/services-portfolio/access-to-products/?option=com_csw&view=details&product_id=SST_GLO_SST_L4_REP_OBSERVATIONS_010_011). To complete the data from 2007 to 2018 another L4 OSTIA product is used, (Bell et al., 2000). Both OSTIA products are merged after a cross validation is performed. The data is available at (http://marine.copernicus.eu/services-portfolio/access-to-products/?option=com_csw&view=details&product_id=SST_GLO_SST_L4_NRT_OBSERVATIONS_010_001). The cross validation of both OSTIA products is done estimating~~. In order to ensure the continuity between both products, As part of the analsys procedure, an estimate of~~ the bias in each ~~of the contributing satellite sensors is made~~satellite productsproduct ~~has been computed. This is done~~ by calculating match-ups between ~~each satellite sensor~~each product and a reference data-set. The details of the procedure can be found in ~~-~~(Bell et al., 2000).. ~~T~~The main difference between NOAA and OSTIA products is that the later uses the in situ data to correct the satellite data, (Roberts-Jones et al., 2012).

2.3 Model data

The outputs from a realistic numerical model are used to perform synthetic observational experiments that help to calibrate the mapping algorithm. The model chosen has been the GLORYS.S2V4 global reanalysis. It is performed with NEMOv3.1 ocean model with a horizontal resolution of 0.25º and 75 vertical z-levels. It is forced by ERA-Interim atmospheric fields (Dee et al., 2011) for the period 1993 to 2015. GLORYS assimilates along track satellite observations of sea level anomaly, sea ice concentration, SST and in situ profiles of temperature and salinity from CORA data base. More details can be found in (Garric and Parent, 2018) and the data is available at (http://marine.copernicus.eu/services-portfolio/access-to-products/?option=com_csw&view=details&product_id=GLOBAL_REANALYSIS_PHY_001_025).

2.4 Data quality control

Prior to the generation of the gridded product it is important to be sure that individual profiles are reliable. In situ profiles in CORA have been quality controlled using an objective procedure and a visual quality control (Cabanes et al., 2013). However, the objective quality control process was originally tuned for the global ocean, therefore requiring an additional review of the profiles inside the region of interest by a visual quality control.

First, we have reviewed all the profiles to remove spikes ~~(zig-zag profiles, profiles with no gradient along the depth), out layers~~ and density inversions. In a second step, we have checked the consistency between the CORA profiles and the profiles collected by KAUST, which are considered to be more reliable as they have been thoroughly analysed by the KAUST data centre with specific criteria adapted to the region. That assessment has been performed separating the Red Sea profiles ~~along with the 1st and 99th quantiles of the KAUST profiles~~ (~~North and South regions in~~ Figure ~~1~~2 left), from the profiles obtained south of the Bab-al-Mandeb strait, (Outer region, see ~~Figure 1~~Figure 1 rigth)~~.~~. In the Red Sea, we also compute the 1% and 99% quantiles of the KAUST dataset (black lines in Figure 2 left), to identify potential outlayers in the CORA dataset. It can be seen that two different regimes appear inside the Red Sea and are clearly identifiable by the temperatures below 500 m. Those profiles located in the Red Sea with temperatures colder than 20ºC below 500 m, show a behaviour which is typical of the outside region, while such pronounced cooling with depth is absent from the KAUST profiles. Thus, those profiles are probably misplaced ~~inside the Red Sea, which coldest temperatures at depth exceeds 20 ºC, were~~and have been rejected.

~~All the profiles in both regions are shown in (Figure 2), along with the 1st and 99th quantiles of the KAUST profiles (only inside the Red Sea, black lines). It can be seen that two different regimes appear inside the Red Sea and are clearly identifiable by the temperatures below 500 m. Those profiles with temperatures colder than 20ºC below 500 m show a behaviour which is typical of the outside region, while such pronounced cooling with depth is absent from the KAUST profiles. Thus, those profiles are~~

Con formato

Con formato
Revisar la ort

~~probably misplaced inside the Red Sea, which coldest temperatures at depth exceeds 20 ºC, were rejected.~~ Finally, f~~F~~or the rest of the profiles, those lying outside a range defined by three times the standard deviation (blue lines in Figure 2) are also rejected.

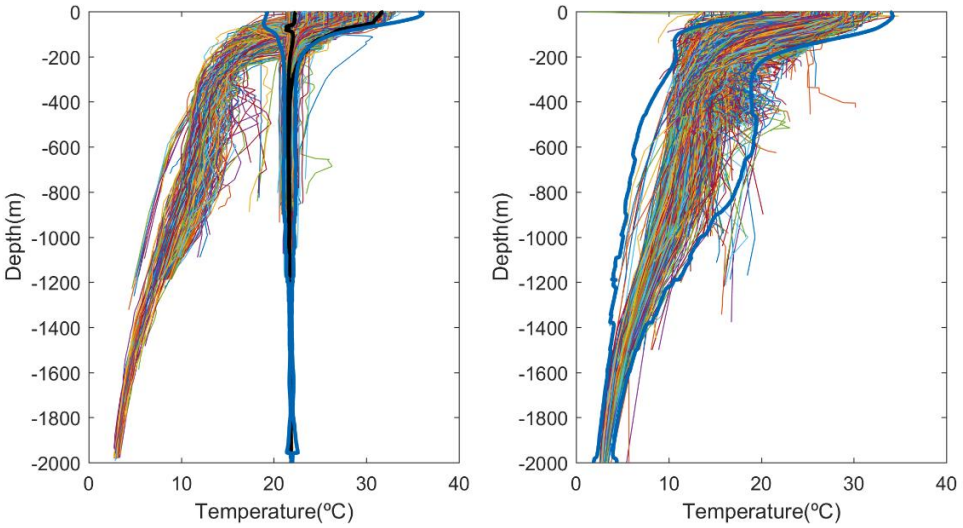

Figure 2: CORA profiles inside the Red Sea (left) and in the outer region (right). The 1st and 99th quantiles of the KAUST profiles are shown in black. The range defined by 3 times the STD of the CORA profiles is shown in blue.

After applying the quality control, ~~11191~~ 10753 profiles are kept inside the Red Sea (82 % of initial profiles) and ~~30522~~ 29906 are kept in the outer zone (88 % of initial profiles). The number of observations per year and per zone is shown in Figure 3~~Figure 3~~. For the outer zone, there is a large number of observations reaching more than 1500 profiles in some years except during the period 1990-2000 in which the number of observations decreased. Regarding the Red Sea, the number of profiles per year in both zones is usually around 200, although in some periods there is a noticeable lack of data (e.g. during the 70s and between 2004 and 2010). In 2001, in the North zone, there is a peak of observations due to an intensive campaign carried out during the summer of that year.

Considering the number of observations per month (Figure 3~~Figure 3~~, Figure SI1), we can see that it remained almost constant through the year in the Southern zone. In contrast, the Northern region is more density sampled in summer, reaching up to more than 1000 observations in July, with roughly 500 observations on average per month during the rest of the year. Regarding the outer zone, the number of observations per month are between 2000 and 3000, with more samples obtained during the first half of the year.

Con formato
Con formato
Revisar la ort
Con formato
Con formato
Revisar la ort

290

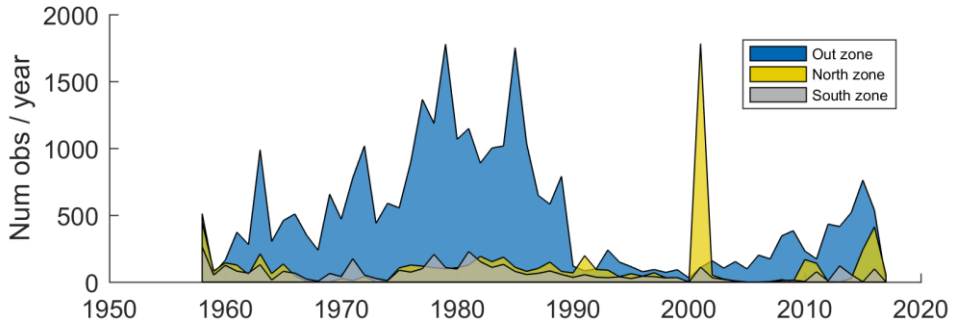
Num obs / year
2000
1500
1000
500
0
1950
1960
1970
1980
1990
2000
2010
2020
Out zone
North zone
South zone

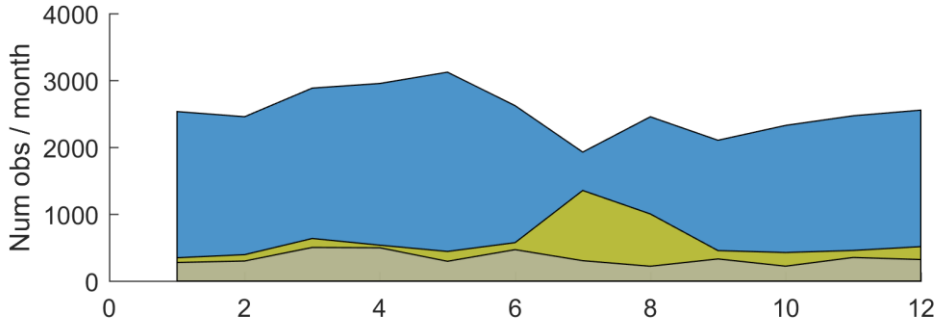
Num obs / month
4000
3000
2000
1000
0
0
2
4
6
8
10
12

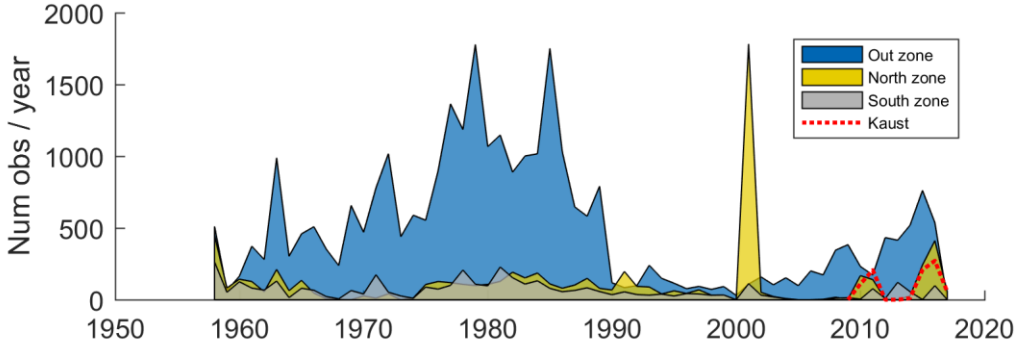
Num obs / year
2000
1500
1000
500
0
1950
1960
1970
1980
1990
2000
2010
2020
Out zone
North zone
South zone
Kaust

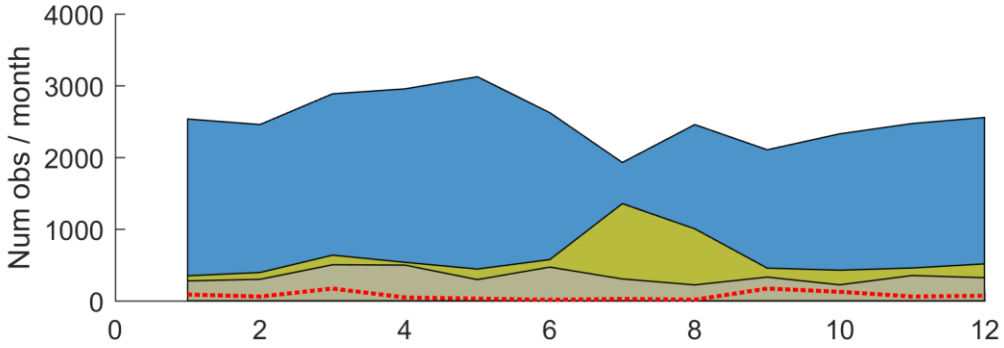
Num obs / month
4000
3000
2000
1000
0
0
2
4
6
8
10
12

Figure 3: Number of observations per year (top). Number of observations per month (bottom). North zone in yellow, South zone in grey and Outer zone in blue. Dashed line (in red) indicates the number of observations coming from the KAUST dataset.

2.5 Mapping Algorithm

In situ observations provide a basis for many oceanographic and meteorological applications. However, the number of observations is limited in space and time and statistical methods must be often applied to homogenize the dataset to be fitted for climate studies and/or model validation (Larsen et al., 2007). We used a classical optimal interpolation algorithm (henceforward OI~~:~~(Gandin, 1965)~~ Gandin et al., XXXX~~) to generate 3D gridded monthly temperature maps from individual in situ profiles (henceforward called TEMPERSEA product).

OI is an algorithm that estimates the optimal value of the field as a linear combination of available observations and a background (i.e. first guess) field, with weights determined from the ~~statistics~~ covariances of observational and background errors. The weights are obtained minimizing the variance of the analysis error (e.g. Jordà & Gomis, 2010). Assuming we have N observations to be mapped into M grid points, the analysed field $\hat{U}$ ~~at a given position r~~ can be written in matrix form as:

$$\hat{U}(r) = BK + S^T * D^{-1} * d \quad (1)$$

Where BK is a M-vector with the background field, S is a NxM matrix containing the covariances of the field between the observation and grid locations, D is a NxN matrix containing the covariances between observations, and d is the N-vector of observed anomalies with respect to the background field:

$$d = y_{obs} - BK(r_{obs}) \quad (2)$$

The observations are not perfect, and assuming that observational errors are not correlated with the true field, the covariance matrix D can be split into the sum of two matrices;

$$D = (B + R) \quad (3)$$

where the elements of B describe the covariance of the true field between pairs of observation points ($B_{ij} = \overline{\tilde{U}(r_i)\tilde{U}(r_j)}$) and R contains the observational error covariances ($R_{ij} = \overline{\varepsilon_i \varepsilon_j}$). In our case we assume observational errors are decorrelated, so R becomes a diagonal matrix with observational error variances in the diagonal. To sum up, the value of the analysis field at point r is given by

$$\hat{U}(r) = BK + S * (B + R)^{-1} * d \quad (4)$$

For convenience, covariance matrices can be transformed to correlation matrices dividing by the field variance $\widetilde{\sigma}^2$ This implies that the diagonal elements in R are now defined as$\gamma_2 = \frac{\varepsilon^2}{\sigma^2}$, the noise-to-signal ratio. The correlations of the field between different locations and times is modelled using a Gaussian function for the spatial component and an exponential por the temporal component:

$$\rho = e^{\frac{-{d_{ij}}^2}{2*L^2}} * e^{\frac{-t_{ij}^2}{T}} \quad (5)$$

Where d_{ij} is the distance between points i, j , and t_{ij} is the time lag.L is the spatial correlation length scale, and T is the time correlation scale.

The parameters, L, T and γ , have been determined from sensitivity experiments using synthetic data. In particular, GLORYS fields are considered as the "truth". Temperature profiles are extracted from GLORYS outputs at the same time and location than the actual profiles were obtained. Then, the mapping algorithm is applied to those synthetic profiles and the outputs from the analysis are compared to the original GLORYS fields. Thus, we can estimate the optimal value for L and γ parameters that minimizes the error of the mapping algorithm provided the characteristics of the observational network and the field variability. The parameter T has been estimated computing the autocorrelation time scale from the GLORYS fields. The analysis is performed over a grid with a spatial resolution of 0.25°x0.25° and 23 vertical depth levels unevenly distributed (Figure 4~~Figure 4~~).

Con formato

Con formato
Revisar la ort

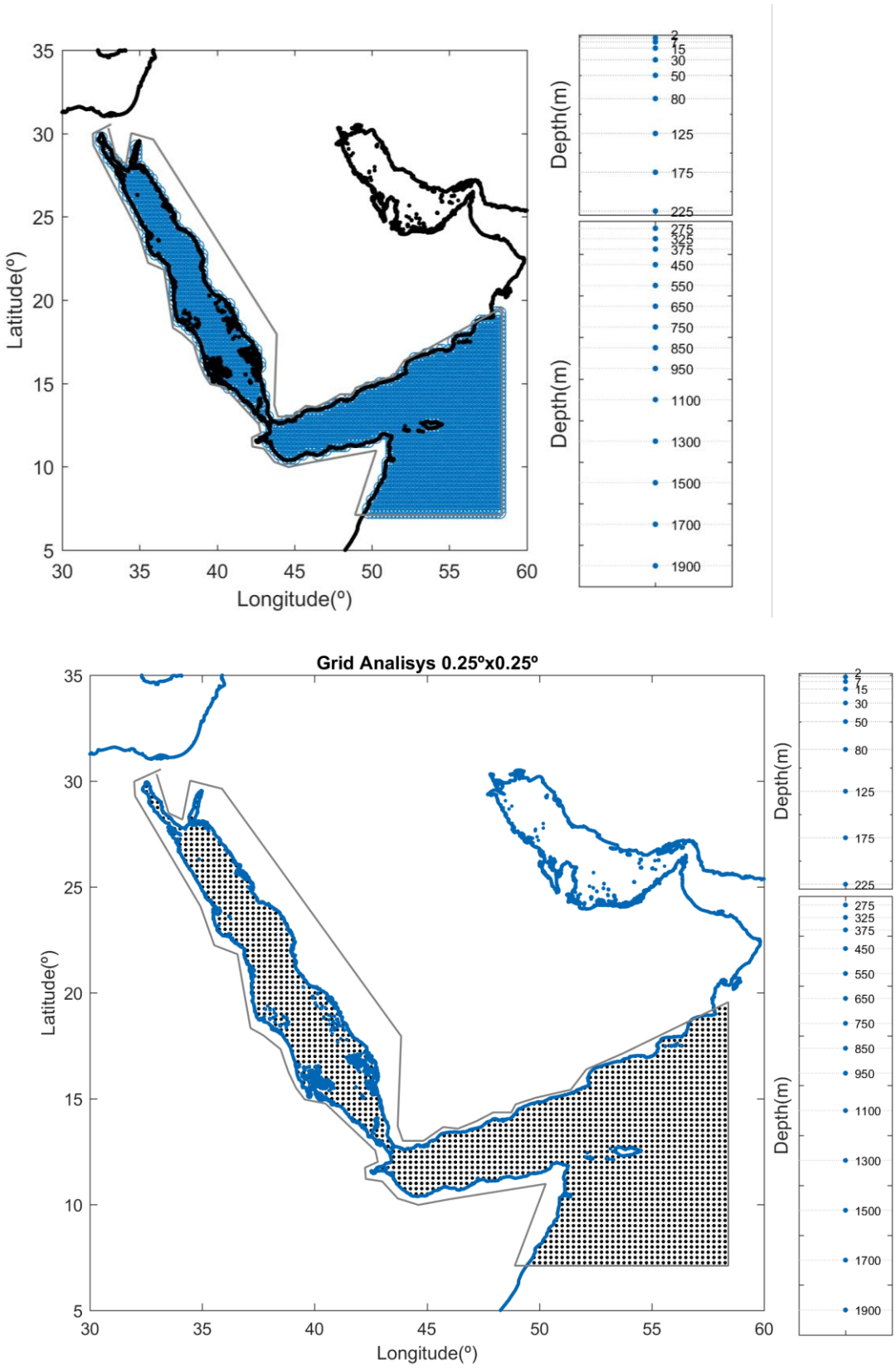

Figure 4: (Left) Analysis grid used in the generation of TEMPERSEA product. (Right) Depth levels.

The background (BK) used in TEMPERSEA is a 12-month climatology. This climatology is computed merging all available observations for each month and then applying the OI algorithm to them. However, the number of profiles is often large and the inversion of the D matrix in (1) can be ill-conditioned when profiles are too close (i.e. at a distance much lower than the correlation length scale). Thus, before the OI algorithm is applied, a data thinning is performed using a K-means algorithm. This clustering technique divides the whole set observations into a predefined number of clusters (Camus et al., 2011). In this case, each cluster represents the mean value of all the observations close to a centroid location. An example is presented in Figure 5~~Figure 5~~. for the month of January. Once we have defined the reduced set of observations grouped per months, the OI algorithm (1) is applied using L_{back} = 150 Km and Υ_{back} = 0,1. No time correlation is considered for the computation of the climatology. Those parameters have been obtained from sensitivity experiments as explained before, which also have shown that the data thinning does not degrade the quality of the background field.

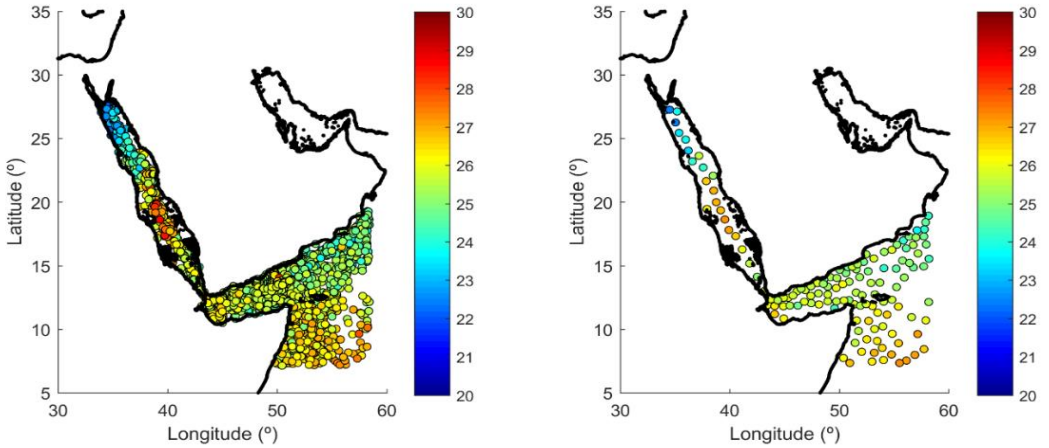

Figure 5: (Left) distribution of all the available observations for January (n=2705). (Right) distribution of observations after applying the K-means algorithm (n=135).

Once the climatology is computed, the analysis is performed on the anomalies with respect to it. Thus, the total temperature is computed as the combination of the background and the analysed anomaly field (see (4)). For months or locations lacking observations the analysis will tend to the deliver background field (i.e. second term in the right-hand side of equation (4) is zero). The parameters used for the analysis are L= 200 km, T= 2 months and γ= 0,1. An example of the results of the analysed temperature anomalies for two consecutive months is shown in Figure 6~~Figure 6~~.

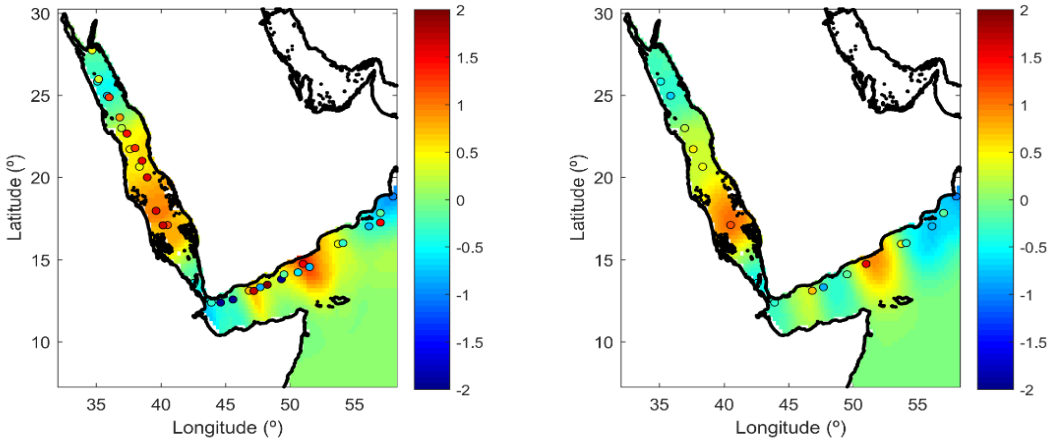

Figure 6: Analysed temperature anomaly field for October 1958 (left) and November 1958 (right). The dots represent the location and value of the observations used in the analysis of each month.

2.6 Product error

One of the advantages of the OI formulation is that it also provides an estimate of the error covariances (or correlations) associated to the analysis. The MxM analysis error covariance matrix $\hat{\sum}$ is given by

$$\hat{\sum} = G - (S^T(B+R)^{-1}S) * \tilde{\sigma}^2 \quad (6)$$

Where the entries of the MxM matrix G are the correlations of the background error between pairs of analysis points, S, B and R have been defined above and $\tilde{\sigma}^2$ is the variance of the field. The latter is estimated from the outputs of GLORYS model. We are particularly interested in the diagonal terms of $\hat{\sum}$, which give the analysis error variance ($\hat{\varepsilon}^2$) at each of the M analysis points.

The formal estimate of the analysis error variance given by (6) depends on the number and distribution of observations as well as on the parameters chosen, but not on the observations themselves. Therefore, it is useful to have a first-order estimate of the accuracy of the formal error estimates. To do so we perform a test using synthetic data from GLORYS outputs. That is, we extract pseudo-observations from GLORYS temperature fields, apply the mapping algorithm as defined above and compare the outputs with the original model fields to obtain the "true" errors. Figure 7a shows the time evolution of the RMS difference between the GLORYS outputs and the background ($\sqrt{\tilde{\sigma}^2}$) averaged per vertical levels, where the ~~std~~ standard deviation (std) of the errors in the background field was used as an estimate of the error in the temperature field. This is an important quantity as it defines the baseline error that our product has in places/times when no observations are available. Error estimates are largest at 125 m depth, with a clear seasonality in the upper layers. Below 300 m the background errors decrease well below 1ºC, except in some periods at 1000 m in which GLORYS data show strong deep anomalies. Concerning the spatial distribution of the background errors (Figure 8a), values average 0.57ºC at 7 m, with higher values along the Arabian coasts and in the Gulf of Aden, where background errors reach 1ºC. At 125 m the averaged background error is 1.12 ºC, with minimum values in the central Red Sea (0.5ºC) and maximum values in the Gulf of Aden (~1.5ºC), where interannual variability is more important and the climatological background is less representative of the temperature field. Figure 7b shows the time evolution of the RMS error of the analysed temperature field is presented. Although the main features seen in the background errors are present, it is clear to that using OI improves the estimate of the temperature field compared with the use of climatology, with a reduction rate ranging from 1.3 to 1.6 (i.e. errors reduced between 30% and 60%). The RMS error maps at 7 m show the averaged value to be reduced to 0.44 ºC, and in most areas the reduction rate is larger than 1.5. At 125 m the RMS error is larger again in the Gulf of Aden but the reduction rate ranges between 1.2 and 1.5. Finally, the formal error estimates are slightly lower (about 20% lower) than the "true" error (Figure 7~~Figure 7~~c and Figure 8~~Figure 8~~ right). However, it is able to capture the seasonality, the maximum at 125 m, and the higher values around 1200 m. The error decreased between 1975 and 1990, due to the higher number of observations distributed in space and time during that period (Figure 7~~Figure 7~~), as also reflected in the "true" error. The formal error replicates the same spatial structure as the "true" error does, both at the surface layer and at 125 m. The magnitude of the formal error is slightly lower than the "true" error (basin averages are 0.31ºC and 0.44ºC, respectively, at the surface, and 0.71ºC and 0.88ºC, at 125 m).

Con formato
Con formato
Revisar la ort
Con formato
Con formato
Revisar la ort
Con formato
Con formato
Revisar la ort

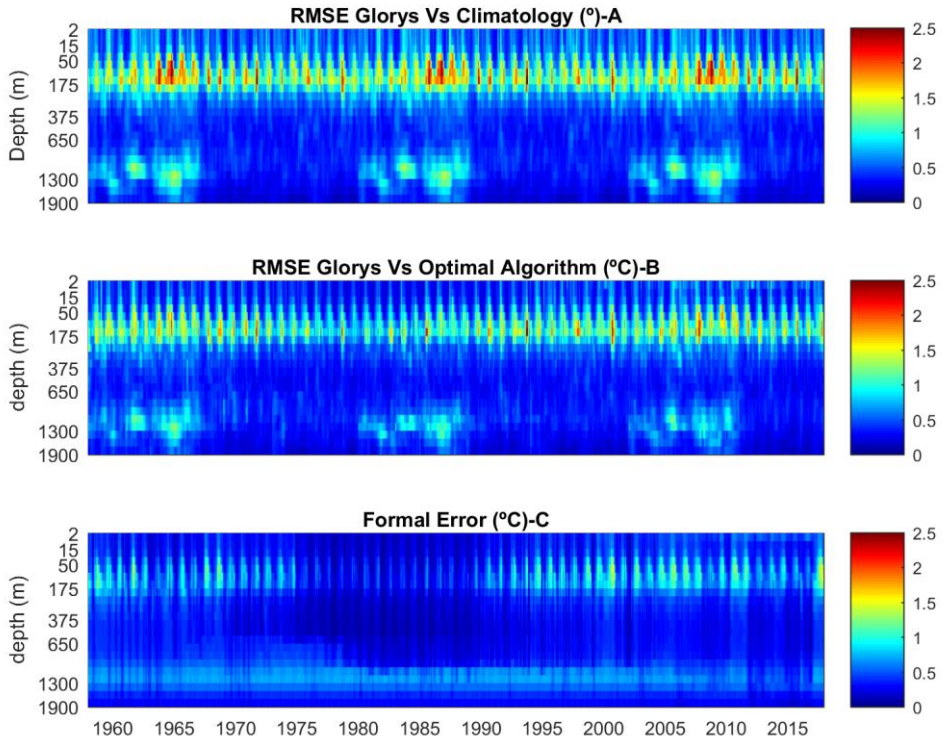
RMSE Glorys Vs Climatology (°)-A
Depth (m)
2
15
50
175
375
650
1300
1900
2.5
2
1.5
1
0.5
0
RMSE Glorys Vs Optimal Algorithm (°C)-B
depth (m)
Formal Error (°C)-C
1960 1965 1970 1975 1980 1985 1990 1995 2000 2005 2010 2015

480

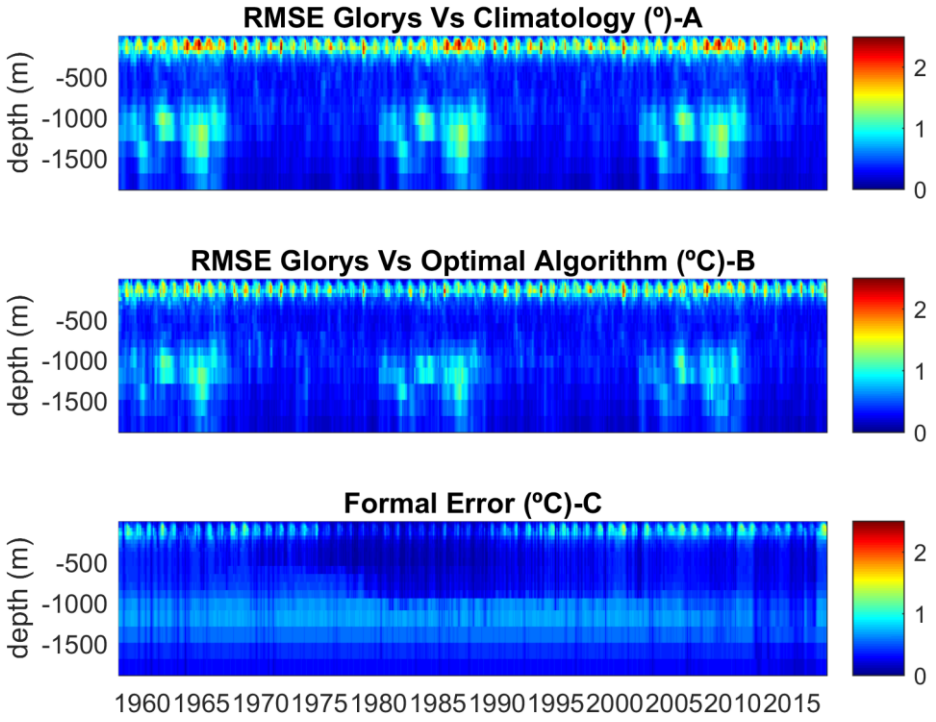
RMSE Glorys Vs Climatology (°)-A
depth (m)
-500
-1000
-1500
2
1
0
RMSE Glorys Vs Optimal Algorithm (°C)-B
Formal Error (°C)-C
1960 1965 1970 1975 1980 1985 1990 1995 2000 2005 2010 2015

Figure 7: (a) Standard deviation ($\sqrt{\widetilde{\sigma^2}}$)of the background errors (in ºC). (b) RMSE (in ºC) of the analysis fields obtained using synthetic data from GLORYS. (c) Formal error ($\sqrt{\widehat{\varepsilon^2}}$, in ºC). Note the vertical axis is distorted to enhance the visualization of the upper layer.

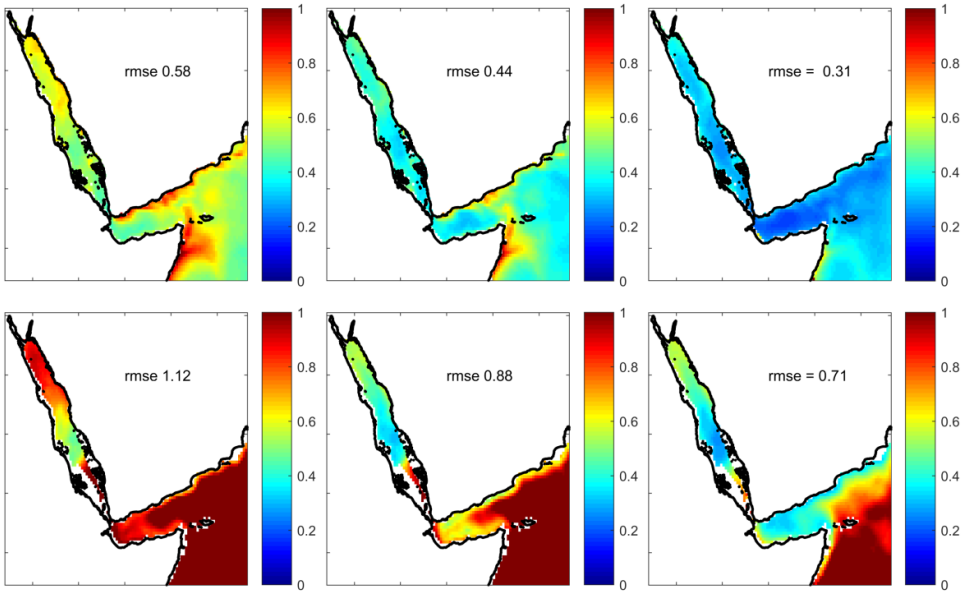

Figure 8: Horizontal distribution of the RMSE (in ºC) of the background (left) and OI (centre), and formal error (right). The results are shown for 7 m depth (top) and 125 m depth (bottom).

Computing the formal error using (6) allows us to derive the formal estimate of the errors when computing regional averages. The formal estimate of the regional average can be computed as:

$$\varepsilon_{av}^2 = \frac{1}{M^2}\sum_{ij} e_i e_j \qquad (8)$$

Where ε_{av}^2 represents the error of the average, M is the length of analysis points and $\sum_{ij} e_i e_j$ is the sum of the error covariances between all the pairs of points included in the averaging. Figure 9~~Figure 9~~ shows the time evolution of the formal estimate of the average temperature in the north zone (in grey) with the "true" error obtained from synthetic observations (in blue). Obviously, the formal error cannot capture the actual error at each month (i.e. is a statistical approximation), but it can be seen that it fits the std of the "true" errors. Also, it is able to identify the periods in which the errors decrease (between 1975-2000) due to the larger density of observations. Therefore, the formal estimate seems to be a reasonable estimate of the analysis error.

Con formato

Con formato
Revisar la ort

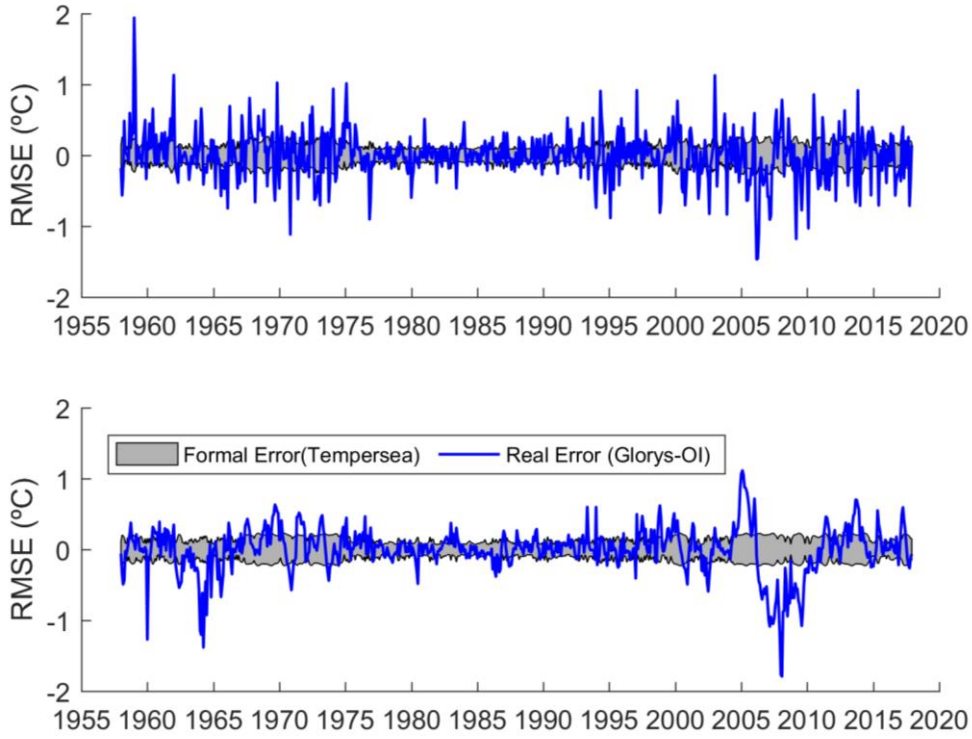

Figure 9: Comparison of the formal error of the temperature average in the North area with the "true" error when the algorithm is applied to synthetic data. Results shown for (a) 7m depth and (b) 125 m depth.

3. Results

3.1 Comparison with satellite results

We compared the first level fields with satellite data from AVHRR and OSTIA as an independent evaluation of the TEMPERSEA product. The monthly variability of regionally averaged temperature anomalies from TEMPERSEA shows good agreement with the satellite estimates (Figure 10~~Figure 10~~). Monthly variations of ~1ºC are captured by all the products as well as variations at lower frequencies. During the periods with few observations the analysis anomalies tend to zero, so the discrepancies with the satellite products increase. The correlation with AVHHR ranges between 0.42 and 0.61 and between 0.39 and 0.51 with OSTIA (Table 1~~Table 1~~). Discarding the periods with few in situ observations (i.e. with formal error > 0.15ºC) the monthly correlations reach 0.67 and 0.61, respectively. Regarding the RMSE the values range between 0.43 and 0.48 ºC for AVHRR and 0.38 and 0.49 ºC for OSTIA. It must be noted that the SST value of TEMPERSEA corresponds to the first level of the product, 2 meters. This level represents the mean value of the profile temperature from the surface to 4 meters of depth. In contrast, the satellite products take the value of the temperature on the first mm of the water column, and consequently the variability of the satellite data is larger than TEMPERSEA. Finally, both satellite estimates, although highly correlated (0.86-0.91) show important discrepancies, with RMS differences of 0.21-0.24ºC (Fig. 10, Table 1).

Con formato
Con formato
Revisar la ort
Con formato
Con formato
Revisar la ort

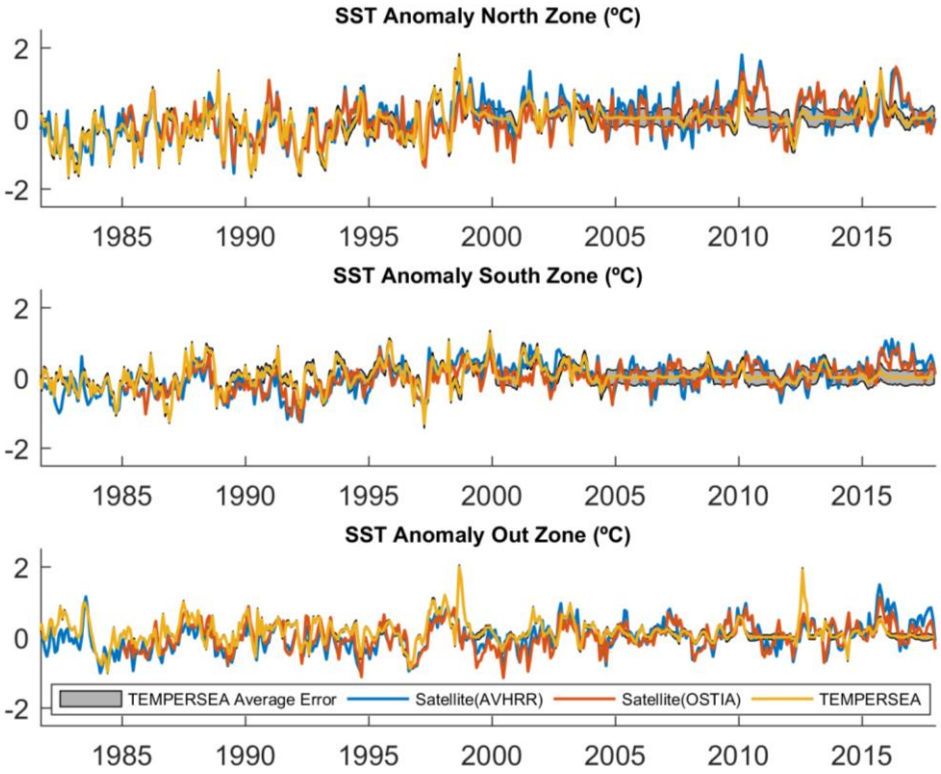

Figure 10: Monthly anomalies of regionally averaged SST in the three zones, north (top), south (middle) and outer (bottom). The three datasets are shown for the common period: Tempersea (yellow line), AVHRR (blue line), OSTIA (red line). The grey patch represents the uncertainties estimated for the TEMPERSEA product.

	North zone		South zone		Outer zone	
	Correlation	RMSE (ºC)	Correlation	RMSE (ºC)	Correlation	RMSE (ºC)
TEMPERSEA - SAT(AVHRR)	0.61(0.67)	0.48(0.47)	0.42(0.48)	0.43(0.48)	0.47(0.58)	0.43(0.44)
TEMPERSEA - SAT(OSTIA)	0.51(0.61)	0.49(0.50)	0.39(0.47)	0.38(0.44)	0.43(0.47)	0.41(0.43)
SAT(AVHRR) - SAT (OSTIA)	0.91	0.24	0.86	0.23	0.87	0.21

Table 1: Statistics of the comparison of regionally averaged SST monthly anomalies between TEMPERSEA, AVHRR and OSTIA. In brackets the values when only periods with enough in-situ observations (i.e. formal error <0.15ºC) are considered.

3.2 Monthly Climatology

We used TEMPERSEA to characterize the thermal regime of the Red Sea. The averaged field at the surface is characterized by temperatures ranging from 25.5°C in the northern part of the Red Sea to 29ºC in the southern part, with a strong gradient at around 20°N (Figure 11~~Figure 11~~a). In the outer region SST's are lower ranging from 26.5°C in the Indian Ocean to 28°C in the Gulf of Aden. Temperatures > 23.5°C are found until a depth of 125 m inside the Red Sea, while only above 50 m in the Gulf of Aden (Figure 11~~Figure 11~~b, c). Below those depths there is a contrasting difference between the two regions, with temperatures in the Red Sea being relatively stable (~22-24°C) through the water column, while

Con formato
Con formato
Revisar la ort
Con formato
Con formato
Revisar la ort

temperature decrease almost linearly with depth in the Gulf of Aden, reach 5ºC at 1500 m depth, due to the oceanic influence (Sofianos et al, 2015).

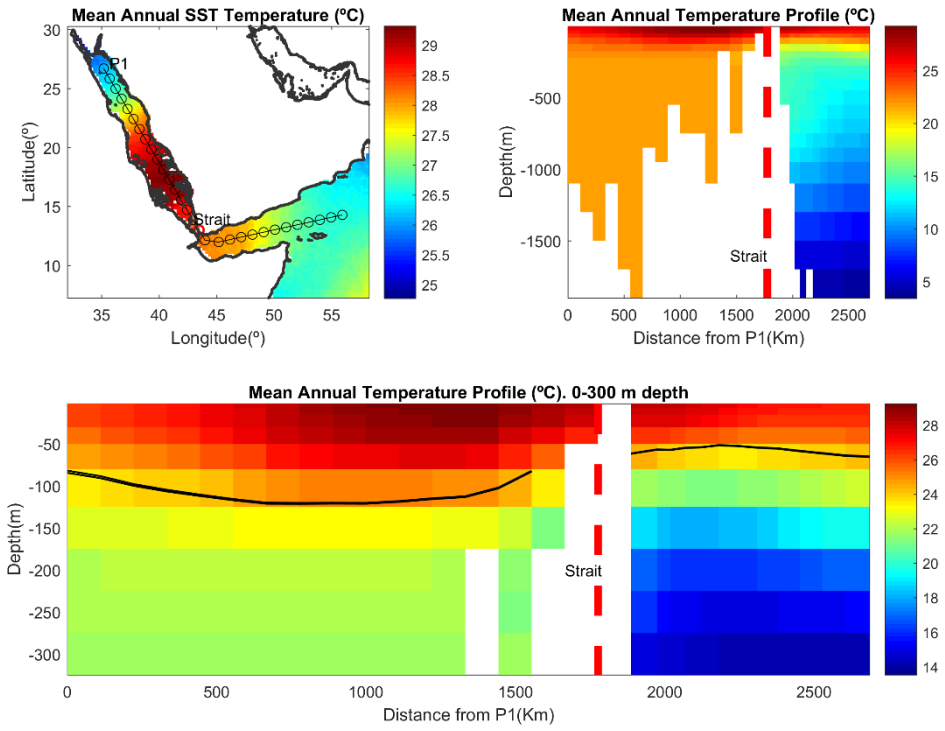

Figure 11: Average temperature from TEMPERSEA computed for the period 1958-2017. (a) Averaged SST. Dots indicate the location of the vertical section shown in the following figures. (b) Vertical section (c) zoom of the vertical section for the upper 300 m. The black line indicates the isotherm of 23.5 °C.

The seasonal thermal evolution in the Red Sea, characterized as the anomaly of the monthly climatology relative to the annual mean, is characterized by negative anomalies in surface temperatures relative to the annual mean reaching -4 ºC in February across the whole basin (Figure 12~~Figure 12~~). Maximum positive anomalies are found in July-August, reaching ~4ºC in the northern part and ~+2-3ºC in the southern part. This implies that the amplitude of the seasonal cycle is larger in the northern than in the southern Red Sea. Minimum negative anomalies with respect to the annual mean in the outer region were found in August (~-2ºC) and maximum anomalies (~+3ºC) are found in May, with both these anomalies being larger in the open ocean than in the Gulf of Aden. These results suggest that the relative minimum found in the Gulf of Aden during summer could be induced by the advection of cold waters from the Indian Ocean.

Con formato

Con formato
Revisar la ort

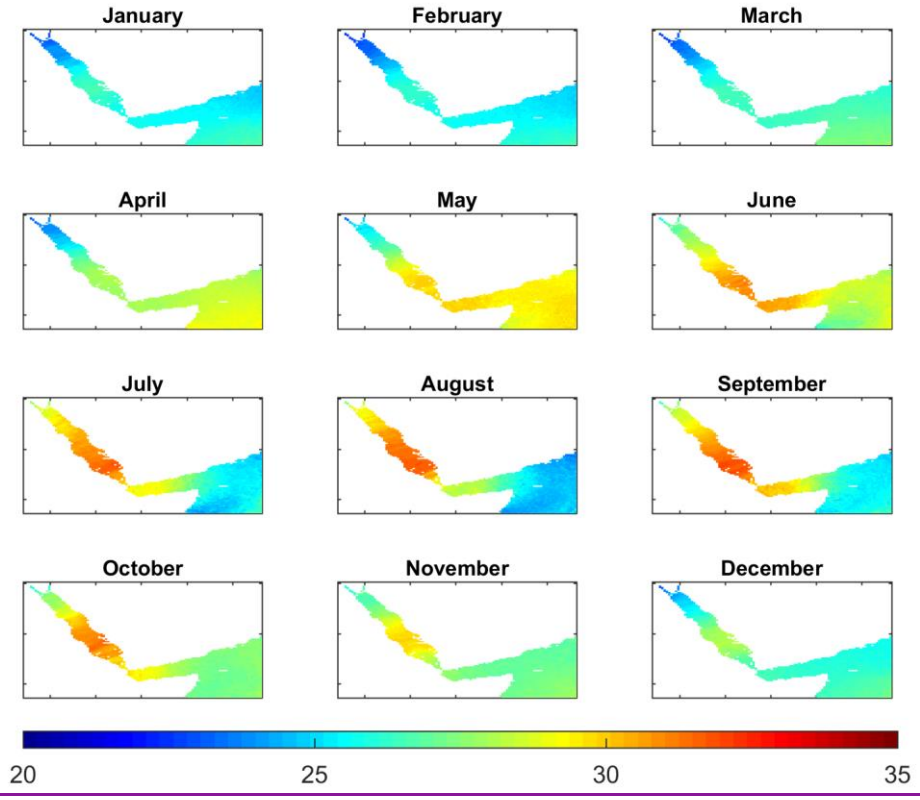
January
February
March
April
May
June
July
August
September
October
November
December
20
25
30
35

620

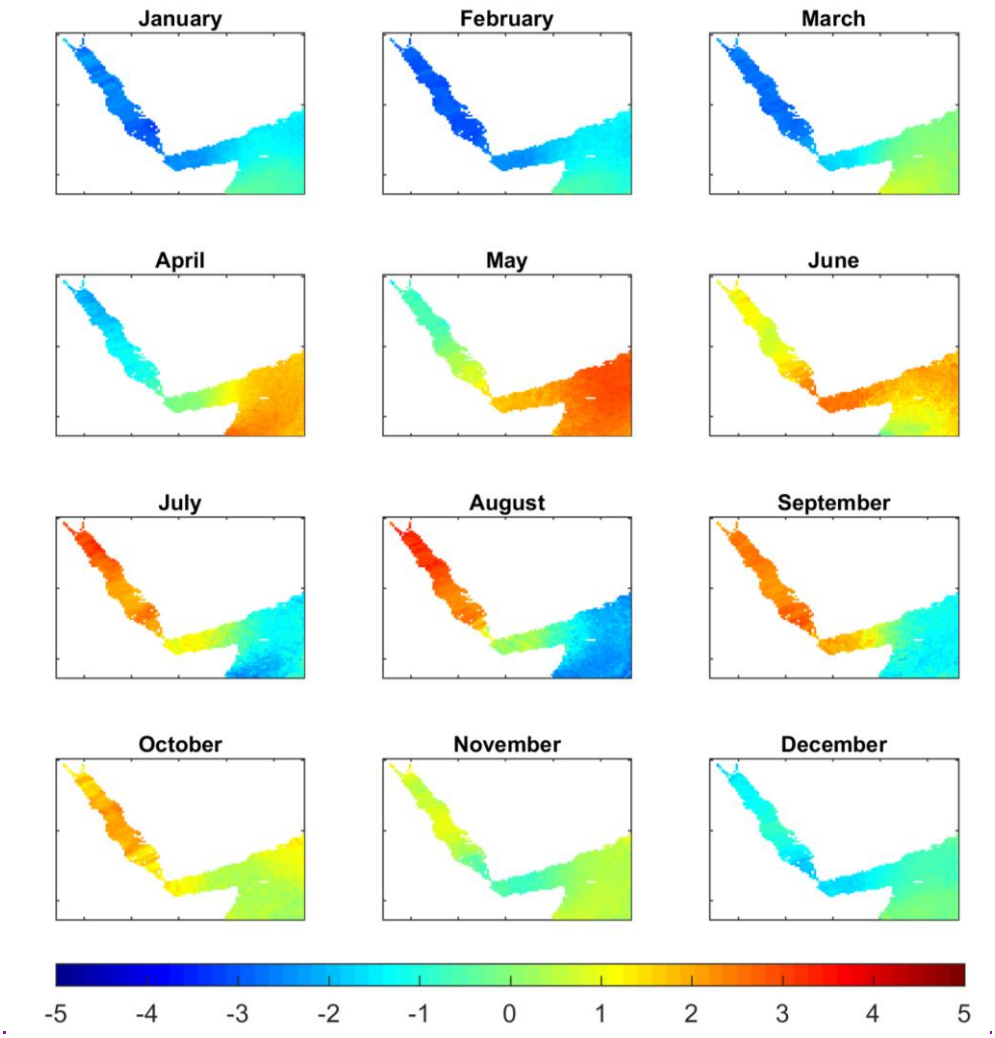

Figure 12: Monthly climatology ~~ical anomalies~~ of the surface temperatures ~~with respect to the annual mean~~ (in ºC). ~~The absolute values are presented in Supplementary Figure XXXX~~

A seasonal thermal regime is only detected above 80-100 m in the Red Sea, being larger in the shallowest layers. In the Red Sea (Gulf of Aden) the larger negative anomalies are found in February (August) and the larger positive anomalies are found in August (May). The Gulf of Aden presents large seasonal variations between 50 and 200 m, with departures from the annual mean range from -4ºC to +4ºC from August/September to April/May.

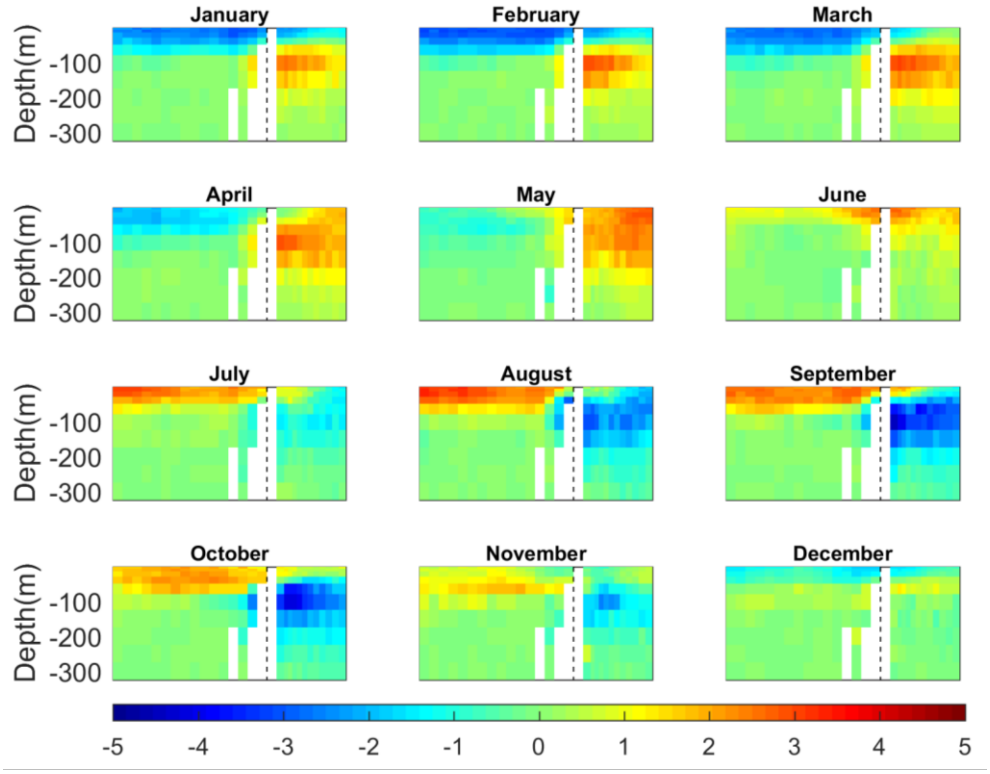

Figure 13: Monthly climatology of temperature anomalies along the section depicted in Figure 11a, with a zoom in the 0-300 m layer.

The seasonal evolution of the depth of the thermocline, defined here as the depth showing the maximum vertical temperature gradient, was computed for each grid point and then averaged regionally (Figure 14~~Figure 14~~). In the Red Sea the thermocline was deeper in February and shallower in the summer months, as expected. However, a clear difference is found between the northern and southern regions. In the northern part the thermocline is deeper, reaching 80 m in February, while in the southern part it is rather constant with monthly-averaged values ranging from 35 m to 50 m. In the outer region, the thermocline is deeper with maximum values of 100 m in March-May and minimum values of 70 m in September-October.

Con formato

Con formato
Revisar la ort

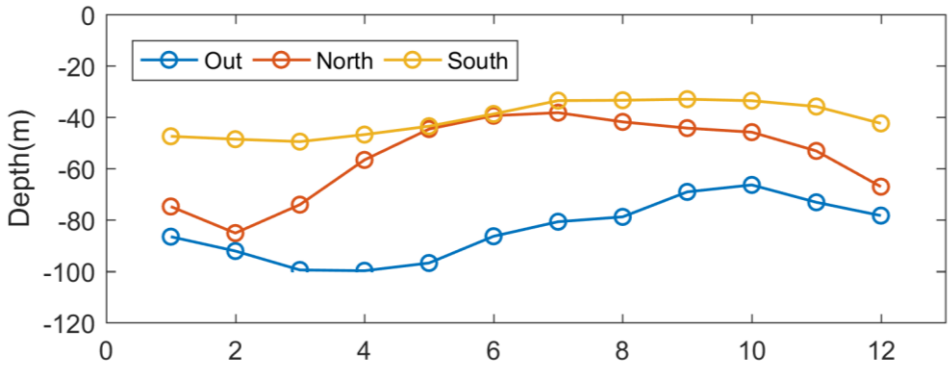

Figure 14: Seasonal evolution of the regionally averaged depth of the thermocline.

3.3 Interannual variability

In the Red Sea, the ~~std~~ standard deviation of interannual variations of the basin averaged temperature at the sea surface and the upper layer (0-100 m) are 0.33 ºC and 0.34 ºC respectively (Figure 15~~Figure 15~~), an order of magnitude lower than the seasonal changes. At the intermediate and bottom layers interannual changes are smaller (0.08 ºC and 0.04ºC, respectively), but in those layers the seasonal variations are negligible, so the relative importance of low frequency changes is larger. In the outer region, interannual changes are larger in all layers (Figure16~~Figure16~~) with a yearly std of 0.38 ºC and 0.45 ºC in the sea surface and the upper layer (0-100m), respectively. In the intermediate layer the interannual std is 0.21 ºC, more than twice larger than in the Red Sea, probably associated to lateral advection of water masses from the Indian Ocean. In the bottom layer, the yearly std is lower, 0.05 ºC, but still larger than in the Red Sea.

To characterize if the interannual variability of the temperature field is the same along the year, we have computed the standard deviation of the time series per months (i.e. 60 values per month; Figure 14). In the Red Sea, the interannual variations are relatively small, with a std ranging from 0.20°C in January to 0.70ºC in November, being quite homogeneous along the basin. In the Gulf of Aden, the interannual variations are larger, particularly from May to November, when std exceeds 1ºC. The rest of the year the std of the interannual variations are smaller (< 0.5ºC).

Con formato

Con formato
Revisar la ort

Con formato

Con formato
Revisar la ort

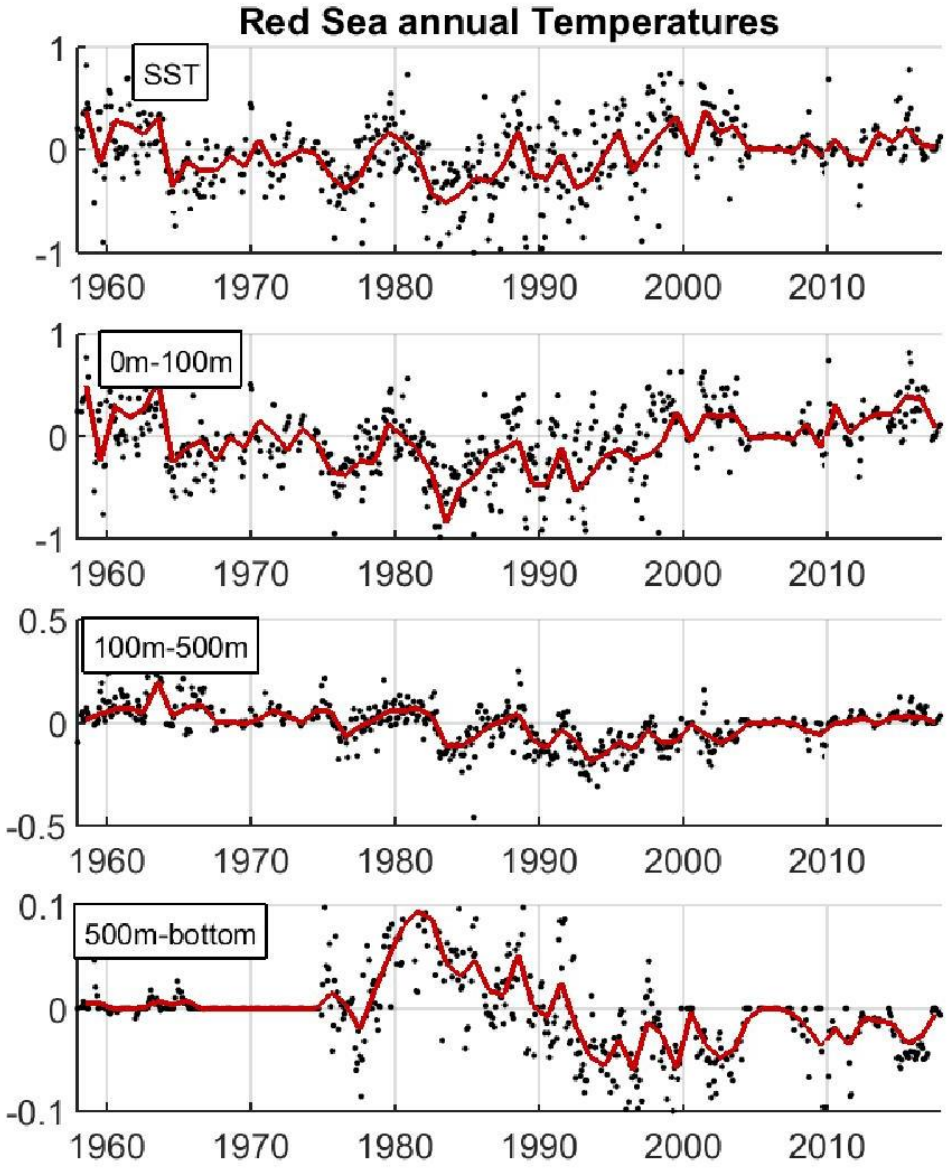

Figure 15: Time series of yearly averaged temperature (in ºC) in different layers (a) SST, (b) 0-100 m, (c) 100-500 m and (d) 500 m - bottom, in the Red Sea. Black dots indicate the monthly values with formal error below 0.2ºC. Note the different vertical axis in each subplot.

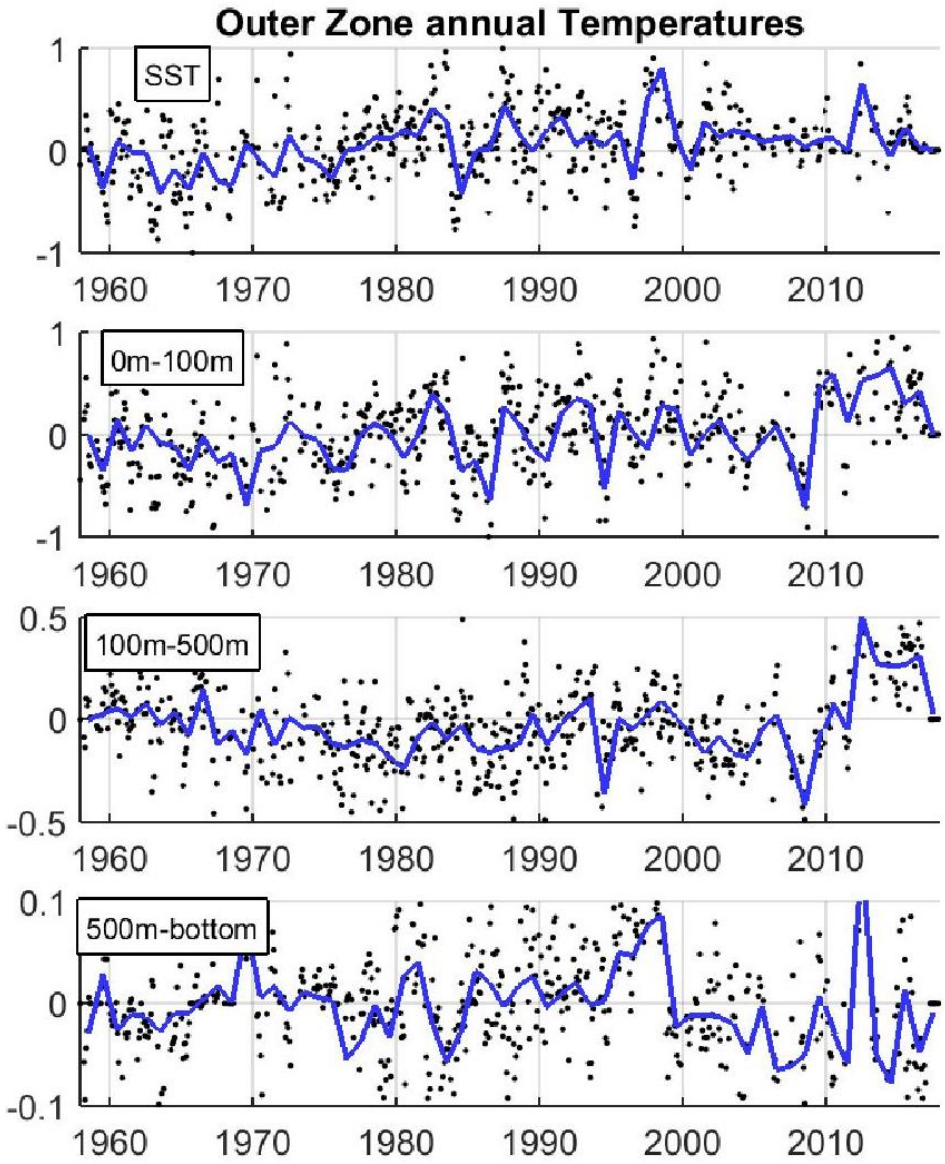

700

Figure16: Time series of yearly averaged temperature (in ºC) in different layers (a) SST, (b) 0-100 m, (c) 100-500 m and (d) 500 m - bottom, in the outer region. Black dots indicate the monthly values with formal error below 0.2ºC. Note the different vertical axis in each subplot.

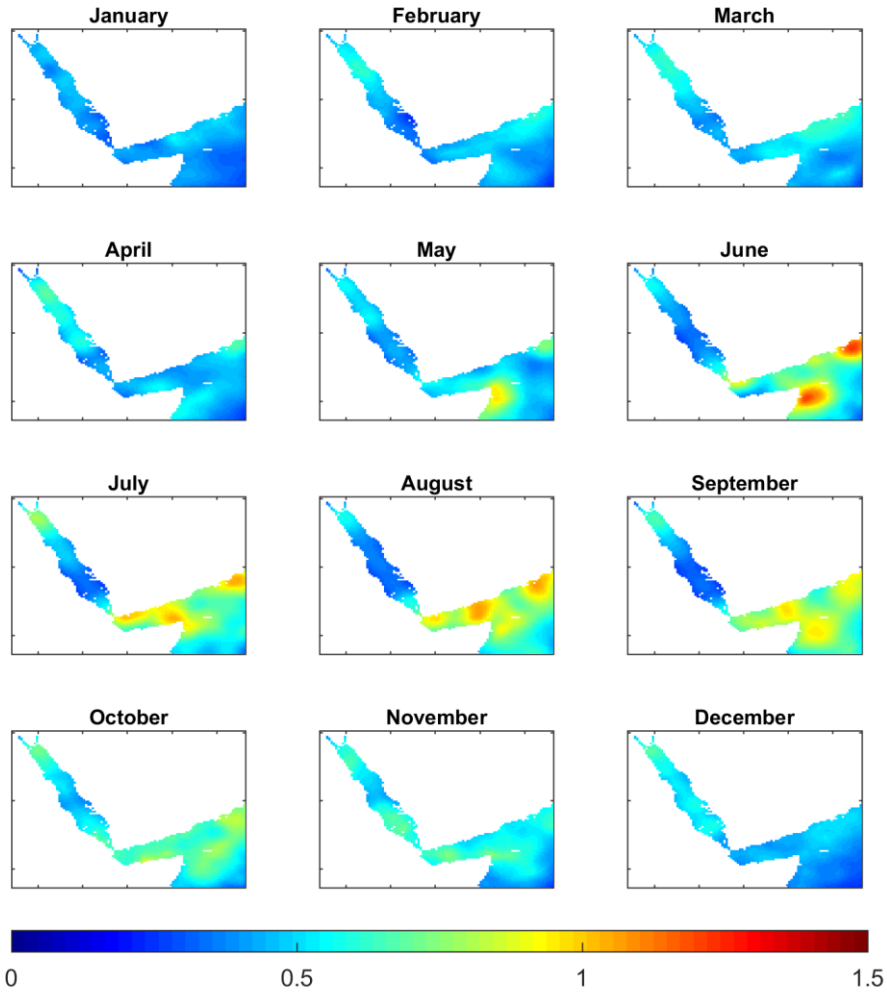

Figure 17: Std of the interannual variations of surface temperature por months (in °C).

In the water column, the largest interannual variations are found in the Gulf of Aden, at the same location where the monthly anomalies were the largest, between 50 and 150 m (Figure 18~~Figure 18~~). The std there even exceeds the values in the surface layer, ranging from 1°C in February to up to 2ºC in September. Inside the Red Sea, the interannual variability decreases with depth, with a std < 0.1ºC below 200 m (Figure 18~~Figure 18~~).

Con formato

Con formato
Revisar la ort

Con formato

Con formato
Revisar la ort

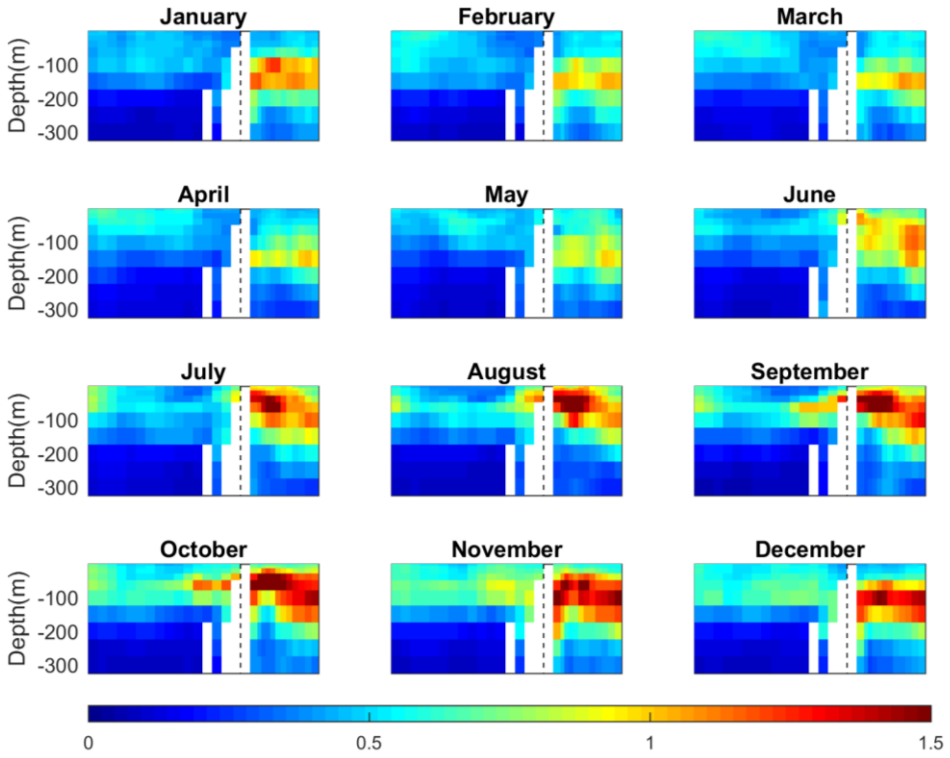

Figure 18 Vertical section along the Red Sea and Gulf of Aden of the std of interannual variations per months (in ºC).

3.4 Multidecadal changes

The assessment of the long-term changes of the temperature field is of paramount relevance as they can shape the characteristics of the local ecosystems and may help characterize the impacts of global warming in the region. Careful examination of the interannual time series suggests that multidecadal changes are over imposed ~~to~~ on the interannual variability. To highlight this, we extract the multidecadal variability applying a moving average with a 10-year window to the monthly time series (Figure 19~~Figure 19~~). In the Red Sea, the low frequency component of the temperature time series in the upper layer show a monotonous decrease from the 1960's reaching a minimum in mid 1980's increasing monotonically since then. In the late 1960's, the temperatures were similar to those in the present decade, both being ~0.4ºC above the minimum. A similar pattern applies to the intermediate layer, but the minimum was reached a decade later, in the mid 1990's. In this case, the difference between the maximum and the minimum was 0.2ºC, with present temperatures ~0.05ºC below those in the 1960's. In the bottom layer the maximum was found in the early 1980's, while a minimum was found at the end of the 1990's. The shift in the multidecadal minima may be reflect heat transfer between layers, but available information is insufficient to assess this possibility.

In the outer region, the low frequency component of the temperature in the upper layer shows an almost regular warming since the 1960's, with a relative minimum in the mid 2000's. In the intermediate layer a more complex behaviour is observed, with two relative minima (in early 1980's and mid 2000's), a relative maximum in the mid 1990's and a clear warming since mid 2000's. The evolution in the deeper layer is similar to the intermediate layer except that no clear warming is observed since the 2000's.

Con formato

Con formato
Revisar la ort

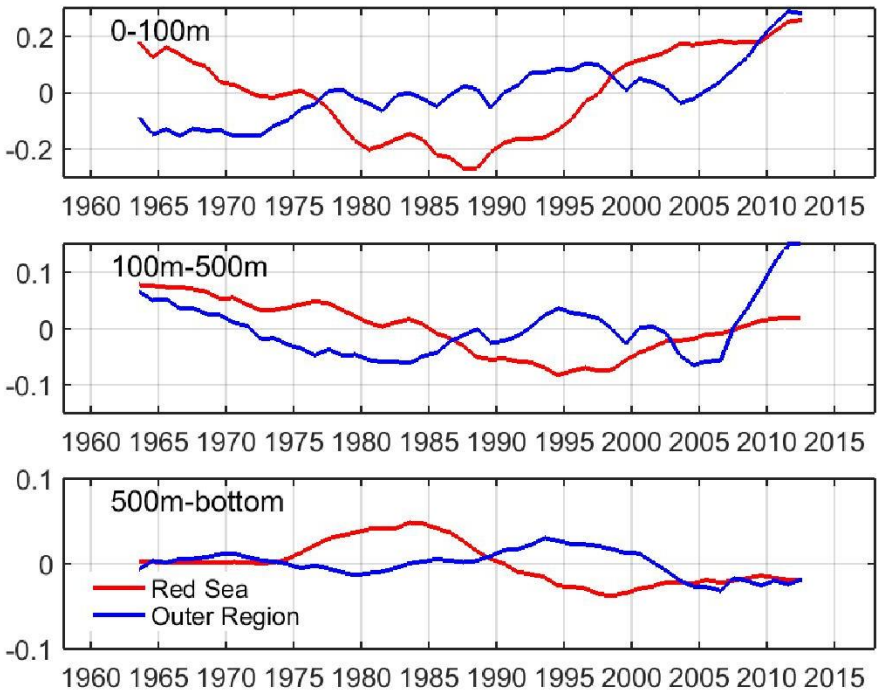

Figure 19: Low-pass filtered temperature time series (in ºC) at different layers in the Red Sea and the Outer Region. A 10-year moving average has been applied to the monthly time series. Note the different vertical axis in each subplot.

Finally, we computed the long-term trends in the Red Sea and the outer region at different depths. To do so, we considered that in some months there were few observations, and therefore analysed temperature anomalies were close to 0. So, in order to avoid biases in the trend estimates, months in which the formal error is greater than 0.15ºC are not considered in the computation.

Trends computed for the whole TEMPERSEA time series (1958-2017; Figure 20~~Figure 20~~a), show only positive trends above 40 m depth, with maximum trends of 0.045 + 0.016 ºC per dec at 15 m, and the largest negative trends at 125 m (-0.072 + 0.011 ºC per dec). In the outer region trends are positive in the whole water column, except between 100 m and 250 m. Maximum trends were found at 15 m (0.12 + 0.01 ºC per dec) and the largest negative trends at 175 m (-0.035 + 0.013ºC per dec). For completeness, we also computed the linear trends for the satellite period (1985-2017; Figure 20~~Figure 20~~b). As the period covered by satellite observations includes the recent period of monotonous warming, trends are positive above 250 m, with maximum values found at 50 m depth (0.27 + 0.04 ºC per dec). The largest negative trends are observed at 400 m (-0.04 + 0.01 ºC per dec). In the outer regions, trends are positive above 800 m, with maximum values at 15 m (0.16 + 0.03ºC per dec).

Con formato
Con formato
Revisar la ort
Con formato
Con formato
Revisar la ort

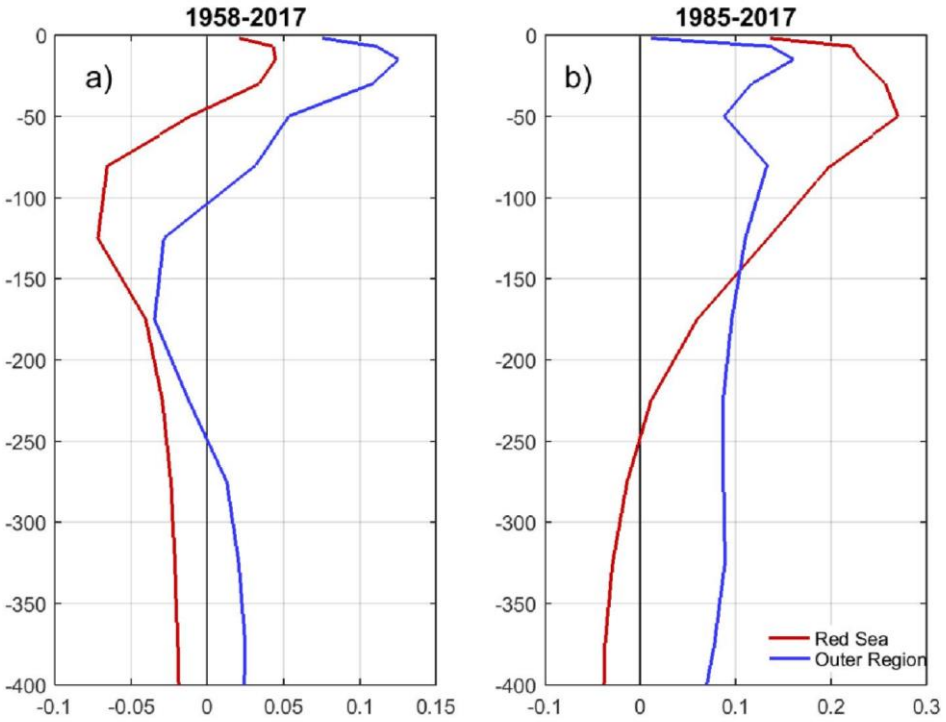

Figure 20: Vertical distribution of temperature trends (in ºC/decade) for the Red Sea (in ~~blue~~red) and the Outer Region (in ~~red~~blue). The linear trends have been computed for the period (a) 1958-2017 and (b) 1985-2017. Note the different horizontal axis in each subplot.

4 Discussion

The TEMPERSEA product provides a homogeneous gridded record of temperature in the whole water column based on quality-controlled in situ observations over the last 60 years. Therefore, it is a valuable complement to the more accurate, but limited on time and depth, satellite-based products. As usual in gridded products, the accuracy of TEMPERSEA is directly linked to the density of in situ profiles, which is rather heterogeneous in space and time. Therefore, us of the TEMPERSEA product should take into account the uncertainty estimates. Our comparison of the formal error estimates and direct estimates based on synthetic experiments suggest that the uncertainty estimates, both at grid point level and for the basin averages, are accurate and are a good indicator of the reliability of the product at a given time/location.

This is especially relevant when long term trends are to be computed. The mapping procedure is a combination of the information provided by the background and by the observations. In cases when/where no observations are available the analysis tends to the background information, which is a monthly climatology that does not change from year to year. This fact artificially damps the estimates of long-term trends (e.g. Llasses, Jordà, & Gomis, 2015), so a careful treatment is needed. Our approach has been to compute trends using only those months that have enough observations (i.e. identified as those with formal error below a certain threshold). Alternatively, (Good et al., 2013), use the analysis of the precedent month as the background field. This allows the propagation of long-term changes and may produce a better estimate of the long-term trends. However, it also may induce spurious trends if sustained periods without observations exist (i.e. several years), so this approach should be careful explored in future analyses of TEMPERSEA.

Another interesting feature of the uncertainty estimate is that it allows identification of sampling strategies that have led in the past to high accuracies, and thus that could be used to guide future

monitoring efforts of Red Sea temperatures. The formal error decreases with the number of observations, but the spatial distribution of the observations also plays an important role. In TEMPERSEA more than 70 months in which the error is as low as 0.1ºC with less than 10 observations have been identified (Figure 21~~Figure 21~~). Conversely, in some months with intensive campaigns more than 500 profiles have been collected, but the formal error did not decrease further. The reason for this is that observations separated less than the typical correlation length scale (i.e. the spatial scale of the process dominating the temperature variability) provide redundant information. On the other hand, we have identified months in which, surprisingly, no observations were gathered in the Red Sea. As mentioned before this represents a serious limitation to accurately quantify long term changes. Therefore, if the goal is to characterize the climatic evolution of the Red Sea temperature an optimized sampling should be designed to minimize the number of required profiles, with approximately less than 10 profiles needed per month. However, this should be repeated monthly, or at least seasonally, to ensure the continuity of the record and to reduce the noise in the long-term change estimates.

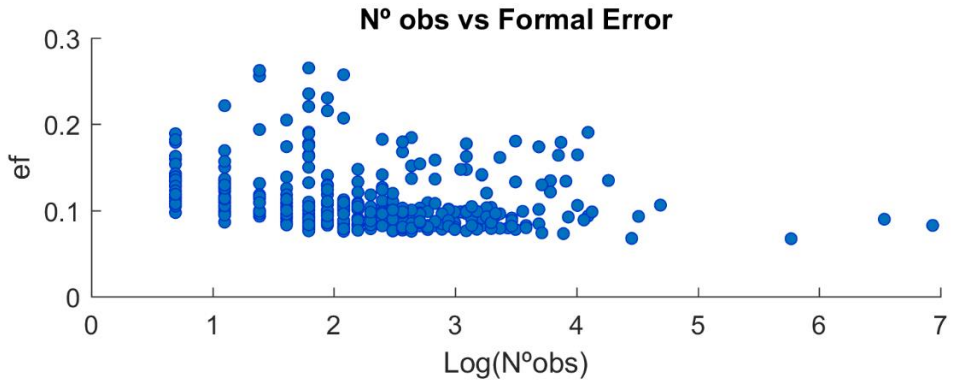

Figure 21: Scatter plot of the formal error vs log of the number of observations per month used to compute the maps.

TEMPERSEA has allowed to characterize the 3D variability of the temperature field in the Red Sea and the adjacent Arabian Sea, which show a different behavior. In the Red Sea most variability is induced by surface processes with little variability at intermediate or deep layers. Conversely, in the Gulf of Aden and the Arabian Sea the influence of lateral advection ~~seems to play~~plays an important role in inducing a shift in the seasonal cycle and large interannual variations in subsurface layers. In order to get a deeper insight in the role of the atmosphere in the sea temperature variations, we analysed air temperatures at 1000 mbars (representative of air in contact with sea surface) and 850 mbars (representative of air masses not directly affected by air-sea interactions, as it corresponds to roughly 1450 m of altitude). In particular we used the output from the JRA55 atmospheric reanalysis for the period 1958-2014 (HARADA et al., 2015), and extend it with the output from the NCEP reanalysis (Kanamitsu et al., 2002) for the period 2014-2017. Before merging both datasets we ensured homogeneity in terms of mean and variance during the common period. The air temperatures have been averaged over the Red Sea and the outer region and compared with the sea temperatures at different layers. In order to isolate the interannual variations we have removed the multidecadal variations using a 10-year moving average high-pass filter.

In the Red Sea the results show a very good correlation between air temperature at 1000 mbar and temperatures at the sea surface and in the 0-100 m layer (correlations of 0.78 and 0.81, respectively; see Figure 2~~Figure 22~~ and Table 2~~Table 2~~). When air temperature at 850 mbar is used, the correlations decrease but are still high (0.68 and 0.69, respectively). This means that most interannual variations in the upper layer of the Red Sea can be explained by large scale changes in air temperature. A non-negligible part (~15% of the variance) can be attributed to air-sea interactions. The effects of atmosphere variability are also detected in the intermediate layer, where the correlation is 0.45. N~~n~~o statistically significant correlations were found in the deeper layers. Concerning the Gulf of Aden, the correlation between air and sea temperatures is lower and restricted to the upper layer (see Table 2~~Table 2~~). This reinforces the

hypothesis that lateral advection plays an important role in driving the interannual variations of temperature in the Gulf of Aden and the Arabian Sea.

	Red Sea		Outer Zone	
	T air 1000 mbar	T air 850 mbar	T air 1000 mbar	T air 850 mbar
Sea Surface	0.78	0.68	0.57	0.47
Sea 0-100m	0.81	0.69	0.43	N/S
Sea 100-500m	0.45	0.37	N/S	N/S
Sea 500 - 1000m	N/S	N/S	N/S	N/S

Table 2: Correlation between air and sea temperatures in the Red Sea and the Outer region. Two heights are used for the air, 1000 mbars, representative of the lower layers of the atmosphere in contact with the sea, and 850 mbars, representative of the temperature in altitude (roughly 1450 m height). Only years with averaged formal error below 0.15ºC are considered. All values are significant at the 95% level (N/S indicated otherwise).

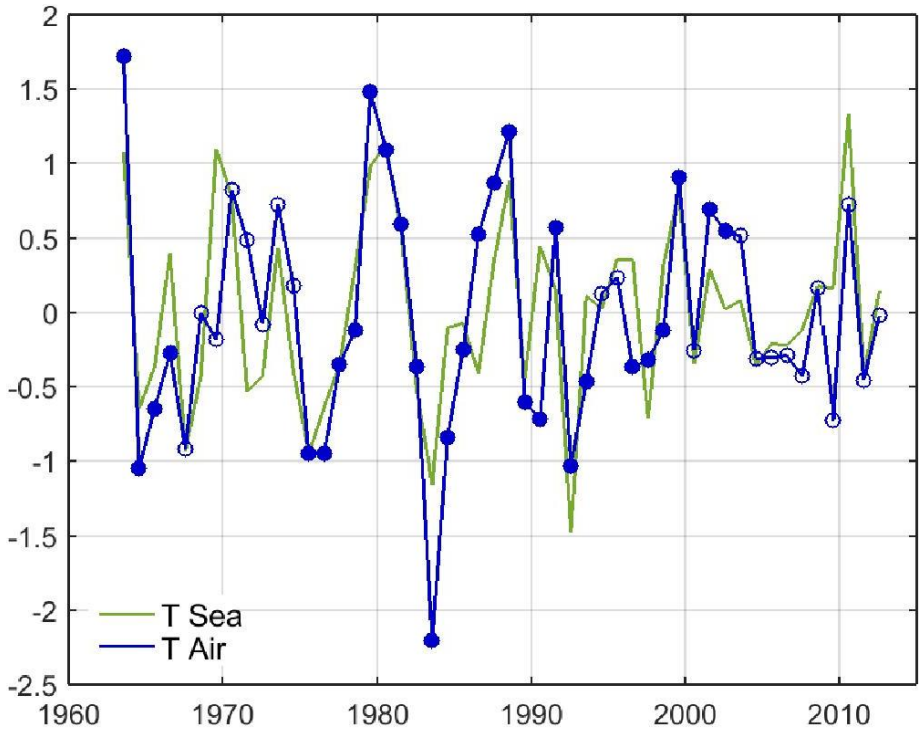

Figure 22: Normalized air temperature at 1000 mbars (green) and 0-100m sea temperature (blue) in the Red Sea. A high-pass filter has been applied to remove multidecadal variations. Solid dots indicate an averaged formal error below 0.15ºC.

Finally, multidecadal changes have been assessed with the TEMPERSEA product showing a non-negligible contribution to temperature variability. This is an important result for the interpretation of long term trends. Linear trends are often computed as an indicator of potential influence of global warming. However, the trends can be masked by low frequency variations when their period is comparable to the

length of the record (Jordà, 2014). This is clear for the temperature records in the Red Sea derived from the TEMPERSEA product. For instance, our results suggest that sea temperature in the upper layer, in the 1960's was similar to the present values, so a very small positive trend is obtained when the period 1958-2017 is used, consistent with recent evidence of long-term thermal oscillations in the Red Sea (Krokos et al., 2019). For the intermediate layer the sign of the trend is even reversed, as the temperatures in the 1960's were higher than those recorded in the recent years. Conversely, if only the last 30 years are considered, which is also the period covered by the satellite record, trends are strong and positive, and therefore easily misinterpreted as linked to global warming. Hence, the conclusions, based on satellite records, that the Red Sea is warming at rates faster than the global ocean (Chaidez et al., 2017; Raitsos et al., 2011), based on the satellite record, need be reconsidered, as warming rates retrieved for 1958-2017 with the TEMPERSEA product are 10 fold lower than those retrieved from satellite records covering the past 30 years.

5 Conclusions

An observational based high resolution and homogeneous 3D temperature product has been developed for the Red Sea for the period 1958-2017 (TEMPERSEA product). For that, two databases of in-situ observations (CORA and KAUST) were merged and quality-controlled, resulting in a dataset of 41713 profiles (11191 in the Red Sea and 30522 in the Gulf of Aden). A mapping procedure based on optimal interpolation has been applied to those profiles to compute two gridded products: a 12-month climatology and a 60-year monthly product. In order to calibrate the algorithm, synthetic data from a realistic numerical model have been used. Furthermore, the formal error from optimal interpolation ~~have~~ has been computed and has proven to be a good approximation to actual uncertainty. The TEMPERSEA product is available from the open data repository Pangea (Agulles et al. 20191).

The product has been compared to satellite observations for the period 1981-2017 showing reasonable agreement in terms of spatial and temporal variability at monthly, seasonal and interannual scales. Also, very good agreement has been found between air temperatures from the atmospheric reanalyses and reconstructed sea temperatures for the whole period 1958-2017, enhancing the confidence on the quality of the product.

The TEMPERSEA product allowed us to characterize the climatology of the temperature in the region. In the Red Sea, the maximum temperatures are found south of 20°N, while the minimum is found in the northern part. Regarding to the seasonal cycle, it peaks in August and is minimum in February. The seasonal cycle is larger in the northern part while in the southern part is smaller in terms of the thermal range in surface waters. In the Gulf of Aden, the phase and shape of the seasonal cycle is different with maximum values in May and minimum values in August. Related to the vertical structure of the temperature field, our results show a large difference between the Red Sea and the Gulf of Aden, especially below the depth of the Bab-El-Mandeb Strait. The Strait isolates the Red Sea allowing it to have temperatures above 20ºC in the whole water column, while the Gulf of Aden, influenced by the open ocean variability show a vertical structure typical of the Indian Ocean, with temperatures reaching 5ºC at 1000 m depth. Furthermore, the length of the product has allowed to characterize multidecadal variability at different layers. Our results show that multidecadal variations have been important in the past and can bias ~~high~~ the trends computed from 30-40 years of data.

TEMPERSEA provides a reference product to describe the temporal evolution of the 3D temperature field in the Red Sea and to calibrate/validate numerical models. This will allow to improve forecasting models and formulate more reliable predictions and climate projections. It has also been shown that the quality of the product is critically linked to the existence of in situ observations. Periods with few observations degrade the quality of the product, so it is important to keep a regular monitoring of the region in order to identify new changes and to remove uncertainties in the climate studies. TEMPERSEA

[1] The data set will be published in Pangea.de upon acceptance of the manuscript

provides a basis to design an optimal sampling program to track the thermal dynamics of the Red Sea. Our results suggest that an effective monitoring can be achieved with few, strategically located, observations.

Acknowledgements

This research was funded by King Abdullah University of Science and Technology (KAUST) through funds provided to S.A. and C.M.D (BAS/1/1072-01-01).

M.A. has been partly funded by the European Union's Horizon 2020 research and innovation programme under grant agreement No 776661 (SOCLIMPACT project).

The TEMPERSEA product is freely available at ~~will be free available at~~ PANGEA repository (www.pangaea.de).

References

Bell, M. J., Forbes, R. M. and Hines, A.: Assessment of the FOAM global data assimilation system for real-time operational ocean forecasting, J. Mar. Syst., 25(1), 1–22, doi:10.1016/S0924-7963(00)00005-1, 2000.

Bongaerts, P., Ridgway, T., Sampayo, E. M. and Hoegh-Guldberg, O.: Assessing the "deep reef refugia" hypothesis: Focus on Caribbean reefs, Coral Reefs, 29(2), 1–19, doi:10.1007/s00338-009-0581-x, 2010.

Cabanes, C., Grouazel, A., Von Schuckmann, K., Hamon, M., Turpin, V., Coatanoan, C., Paris, F., Guinehut, S., Boone, C., Ferry, N., De Boyer Montégut, C., Carval, T., Reverdin, G., Pouliquen, S. and Le Traon, P. Y.: The CORA dataset: Validation and diagnostics of in-situ ocean temperature and salinity measurements, Ocean Sci., 9(1), 1–18, doi:10.5194/os-9-1-2013, 2013.

Camus, P., Mendez, F. J., Medina, R. and Cofiño, A. S.: Analysis of clustering and selection algorithms for the study of multivariate wave climate, Coast. Eng., 58(6), 453–462, doi:10.1016/j.coastaleng.2011.02.003, 2011.

Chaidez, V., Dreano, D., Agusti, S., Duarte, C. M. and Hoteit, I.: Decadal trends in Red Sea maximum surface temperature, Sci. Rep., 7(1), 1–8, doi:10.1038/s41598-017-08146-z, 2017.

Dee, D. P., Uppala, S. M., Simmons, A. J., Berrisford, P., Poli, P., Kobayashi, S., Andrae, U., Balmaseda, M. A., Balsamo, G., Bauer, P., Bechtold, P., Beljaars, A. C. M., van de Berg, L., Bidlot, J., Bormann, N., Delsol, C., Dragani, R., Fuentes, M., Geer, A. J., Haimberger, L., Healy, S. B., Hersbach, H., Hólm, E. V., Isaksen, L., Kållberg, P., Köhler, M., Matricardi, M., Mcnally, A. P., Monge-Sanz, B. M., Morcrette, J. J., Park, B. K., Peubey, C., de Rosnay, P., Tavolato, C., Thépaut, J. N. and Vitart, F.: The ERA-Interim reanalysis: Configuration and performance of the data assimilation system, Q. J. R. Meteorol. Soc., 137(656), 553–597, doi:10.1002/qj.828, 2011.

Eladawy, A., Nadaoka, K., Negm, A., Abdel-Fattah, S., Hanafy, M. and Shaltout, M.: Characterization of the northern Red Sea's oceanic features with remote sensing data and outputs from a global circulation model, Oceanologia, 59(3), 213–237, doi:10.1016/j.oceano.2017.01.002, 2017.

Gandin, L. S.: 49709239320_Ftp.Pdf, , 1965, 1965.

Good, S. A., Martin, M. J. and Rayner, N. A.: EN4: Quality controlled ocean temperature and salinity profiles and monthly objective analyses with uncertainty estimates, J. Geophys. Res. Ocean., 118(12), 6704–6716, doi:10.1002/2013JC009067, 2013.

HARADA, Y., EBITA, A., OTA, Y., ONOGI, K., TAKAHASHI, K., ENDO, H., MIYAOKA, K., KOBAYASHI, S., ONODA, H., MORIYA, M., KAMAHORI, H. and KOBAYASHI, C.: The JRA-55 Reanalysis: General Specifications and Basic Characteristics, J. Meteorol. Soc. Japan. Ser. II, 93(1), 5–48, doi:10.2151/jmsj.2015-001, 2015.

Ishii, M. and Kimoto, M.: Reevaluation of historical ocean heat content variations with time-varying XBT and MBT depth bias corrections, J. Oceanogr., 65(3), 287–299, doi:10.1007/s10872-009-0027-7, 2009.

Jordà, G.: Journal of Geophysical Research : Oceans, J. Geophys. Res. Ocean., 2121–2128, doi:10.1002/jgrc.20224, 2014.

Jordà, G. and Gomis, D.: Accuracy of SMOS level 3 SSS products related to observational errors, IEEE Trans. Geosci. Remote Sens., 48(4 PART 1), 1694–1701, doi:10.1109/TGRS.2009.2034259, 2010.

Kanamitsu, M., Ebisuzaki, W., Woollen, J., Yang, S.-K., Hnilo, J. J., Fiorino, M. and Potter, G. L.: NCEP-DOE AMIP-II Renalalysys (R-2), Bull. Am. Meteorol. Soc., 83(11), 1631–1643, doi:10.1175/BAMS-83-11, 2002.

Karnauskas, K. B. and Jones, B. H.: The Interannual Variability of Sea Surface Temperature in the Red Sea From 35 Years of Satellite and In Situ Observations, J. Geophys. Res. Ocean., 123(8), 5824–5841, doi:10.1029/2017JC013320, 2018.

Krokos, G., Papadopoulos, V. P., Sofianos, S. S., Ombao, H., Dybczak, P. and Hoteit, I.: Natural Climate Oscillations may Counteract Red Sea Warming Over the Coming Decades, Geophys. Res. Lett., 46(6), 3454–3461, doi:10.1029/2018GL081397, 2019.

Larsen, J., Høyer, J. L. and She, J.: Validation of a hybrid optimal interpolation and Kalman filter scheme for sea surface temperature assimilation, J. Mar. Syst., 65(1-4 SPEC. ISS.), 122–133, doi:10.1016/j.jmarsys.2005.09.013, 2007.

Lima, F. P. and Wethey, D. S.: Three decades of high-resolution coastal sea surface temperatures reveal more than warming, Nat. Commun., 3, 1–13, doi:10.1038/ncomms1713, 2012.

Llasses, J., Jordà, G. and Gomis, D.: Skills of different hydrographic networks in capturing changes in the Mediterranean Sea at climate scales, Clim. Res., 63(1), 1–18, doi:10.3354/cr01270, 2015.

Neumann, A. C. and McGill, D. A.: Circulation of the Red Sea in early summer, Deep Sea Res., 8(3–4), 223–235, doi:10.1016/0146-6313(61)90023-5, 1961.

Patzert, W. C.: Wind-induced reversal in Red Sea circulation, Deep. Res. Oceanogr. Abstr., 21(2), 109–121, doi:10.1016/0011-7471(74)90068-0, 1974.

Poloczanska, E. S., Burrows, M. T., Brown, C. J., García Molinos, J., Halpern, B. S., Hoegh-Guldberg, O., Kappel, C. V., Moore, P. J., Richardson, A. J., Schoeman, D. S. and Sydeman, W. J.: Responses of Marine Organisms to Climate Change across Oceans, Front. Mar. Sci., 3(May), 1–21, doi:10.3389/fmars.2016.00062, 2016.

Raitsos, D. E., Hoteit, I., Prihartato, P. K., Chronis, T., Triantafyllou, G. and Abualnaja, Y.: Abrupt warming of the Red Sea, Geophys. Res. Lett., 38(14), 1–5, doi:10.1029/2011GL047984, 2011.

Roberts-Jones, J., Fiedler, E. K. and Martin, M. J.: Daily, global, high-resolution SST and sea ice reanalysis for 1985-2007 using the OSTIA system, J. Clim., 25(18), 6215–6232, doi:10.1175/JCLI-D-11-00648.1, 2012.

Thorne, K. S., Wheeler, J. A., Francisco, S., Wieman, C. E., Ertmer, W., Schleich, W. P., Rasel, E. M., Diego, S., Chung, K. Y., Chu, S., Scully, M. O., Physics, A., Grynberg, G., Stora, R., Pavlis, E. C. and Wheeler, J. A.: References and Notes 1., , 327(June), 1543–1548, doi:10.1126/science.1206034, 2010.

Sofianos, S. and Jhons, W.E, 2015. Water Mass Formation, Overturning Circulation and the Exchange of the Red Sea With the Adjacent Basins. https://doi.org/10.1007/978-3-662-45201-1_20